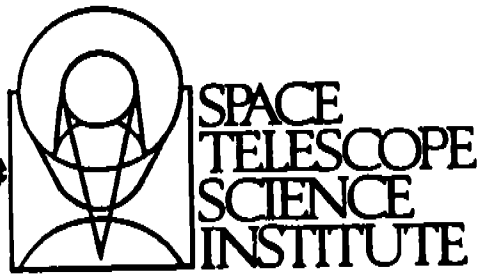

MASTER
Kinney

Hubble Space Telescope

Faint Object Spectrograph

Instrument Handbook

Version 4.0
February 1993

Revision History

Handbook Version 1.0	October 1985; edited by Holland C. Ford
Handbook Version 1.1	May 1990; edited by Holland C. Ford; supplement by G. F. Hartig
Handbook Version 2.0	April 1992; edited by Anne L. Kinney
Handbook Version 4.0	February 1993; edited by Anne L. Kinney

The Space Telescope Science Institute is operated by the Association of Universities for Research in Astronomy, Inc., for the National Aeronautics and Space Administration.

FAINT OBJECT SPECTROGRAPH

INSTRUMENT HANDBOOK

A.L. Kinney

Space Telescope Science Institute
3700 San Martin Drive
Baltimore, MD 21218

Version 4.0
February 1993

Table of Contents

List of Figures

C.1 ~~Figure~~ Description
~~From~~ Spectrum ~~compared with~~
from G2V star model atmosphere.

C.2 FOS spectrum of G2V star
showing ~~with~~ scattering (light contribution).

List of Tables

C.1 Scattered Light Contributions for stars.

INTRODUCTION

The Faint Object Spectrograph and its use is fully described in the Version 1.0 FOS Instrument Handbook (Ford 1985), and in the supplement to the Instrument Handbook (Hartig 1989), from which much of this handbook is drawn. The detectors are described in detail by Harms *et al.* (1979) and Harms (1982).

This version of the FOS Instrument Handbook is for the corrected telescope, after the installation of the Corrective Optics (COSTAR). The main differences in the post-COSTAR FOS are the changes in throughput, changes in efficiency due to the extra reflections of the COSTAR optics, and the change in focal length. The changes in throughput affect all exposure time calculations, and improve the spectral resolution. The extra reflections of COSTAR decreases the efficiency by $10 - 20\%$. The change in focal length affects the aperture sizes. The aperture designations which are already in use both in the Exposure Logsheets and in the Project Data Base (PDB) will not be changed. Apertures will be referred to by their size, followed by the designation used on the Exposure Logsheet. For example, the largest circular aperture will be referred to as the $0.9''$ (`1.0`) aperture, while the largest paired aperture will be referred to as the $0.9''$ paired (`1.0-PAIR`) aperture.

Section 1 presents all information that is needed for proposing to observe with the FOS, *i.e.* **for filling out Phase I Proposals.** The overall instrument capabilities are described and presented in Table 1.0.1. The spectral resolution is in Section 1.1 as a function of grating and aperture. The data for calculating exposure times are in Section 1.2 in three different ways. The easiest way to calculate exposure time is by simply reading off the (simulated) counts s^{-1} $diode^{-1}$ in a grating when illuminated by a constant input spectrum of $F = 1.0 \times 10^{-14}$ erg cm^{-2} s^{-1} $Å^{-1}$ (Figure 1.2.3). The count rate can then be normalized to the expected incident flux of the object of interest. The limits for the brightest objects that can be observed with FOS are in Section 1.3. A discussion of time resolution with the FOS, *i.e.* `ACCUM`, `RAPID`, and `PERIOD` modes, is given in Section 1.4. Polarization is discussed in Section 1.5. The FOS noise and dynamic range are discussed in Section 1.6.

Section 2 presents information that is needed for observing with the FOS after winning HST time, *i.e.* **for filling out Phase II Proposals.** The acquisition of targets is described in Section 2.1. Examples of the Exposure Logsheets that have been validated by the Remote Proposal Submission System (RPSS) are given for target acquisition modes (for example, `ACQ/BINARY`), for the standard data taking mode (`ACCUM`), for the time resolved mode (`RAPID`), and for spectropolarimetry (observed in `ACCUM` mode with the optional parameter `STEP-PATT = POLSCAN`). The Exposure Logsheets can be copied from anonymous ftp (stsci.edu, or 130.167.1.2). The Logsheets are in the subdirectory proposer/documents/props_library, and are called fos_handbook4_example. Caveat emptor.

Section 3. briefly describes the current wavelength calibration, absolute photometry, and flat field calibrations of FOS. The data used to produce the flat fields are shown.

Section 4. describes how to simulate FOS spectra with the "synphot" package which runs in the ST Data Analysis System (STSDAS) under IRAF. A version of the simulator compatible with VAX/VMS machines (XCAL) is also available to be copied from the anonymous ftp account on stsci.edu. The simulators, developed by K. Horne, ~~are useful tools since they~~ allow input of a large variety of spectra, and they incorporate the current calibration files for the FOS.

The ~~actual~~ details of taking data are given in Appendix A, along with the FOS observing parameters both in the nomenclature of Exposure Logsheets, and in the nomenclature of FOS headers. Appendix A gives the equations for calculating the start time of any time

resolved exposure. Appendix B lists the dead diode tables of January 18, 1993. Appendix C is a comparison of GHRS and FOS sensitivities by Gilliland & Hartig (1991). Appendix D summarized the results of tests of scattered red light into the blue side detectors by Caldwell & Cunningham (1992). Observing red objects in the ultraviolet with FOS can be problematical because of scattered red light. Appendix E is a compendium of FOS calibration reports issued by the FOS team since launch, including the science verification reports. Calibration reports can be obtained by requesting copies of Nancy Fulton (see below). Appendix F contains Exposure Logsheets with examples of different FOS modes.

The FOS Instrument Scientists and relevant ST ScI contacts are:

Tony Keyes	410-338-4975	keyes@stsci.edu
Anne Kinney	410-338-4831	kinney@stsci.edu
Anuradha Koratkar	410-338-4470	koratkar@stsci.edu
Nancy Fulton	410-338-4955	fulton@stsci.edu
User Support Branch	410-338-4470	

1. INSTRUMENT CAPABILITIES

The general traits of FOS blue side (FOS/BL) and red side (FOS/RD) are given in Table 1.0.1, along with those of the GHRS for comparison. For further reference, Appendix C contains the ST ScI Newsletter article by Gilliland & Hartig (1991) *A Comparison of GHRS and FOS Sensitivities*.

The Faint Object Spectrograph has two Digicon detectors with independent optical paths. The Digicons operate by accelerating photoelectrons emitted by the transmissive photocathode onto a linear array of 512 diodes. The individual diodes are 0.31″ wide along the dispersion direction and 1.21″ tall perpendicular to the dispersion direction. The detectors span the wavelength range on the blue side from 1150Å to 5400Å (FOS/BL) and on the red side from 1620Å to 8500Å (FOS/RD). The quantum efficiency of the two detectors is shown in Figure 1.0.1. The optical diagram for the FOS is given in Figure 1.0.2. The FOS entrance apertures are 3.6′ from the optical axis of HST.

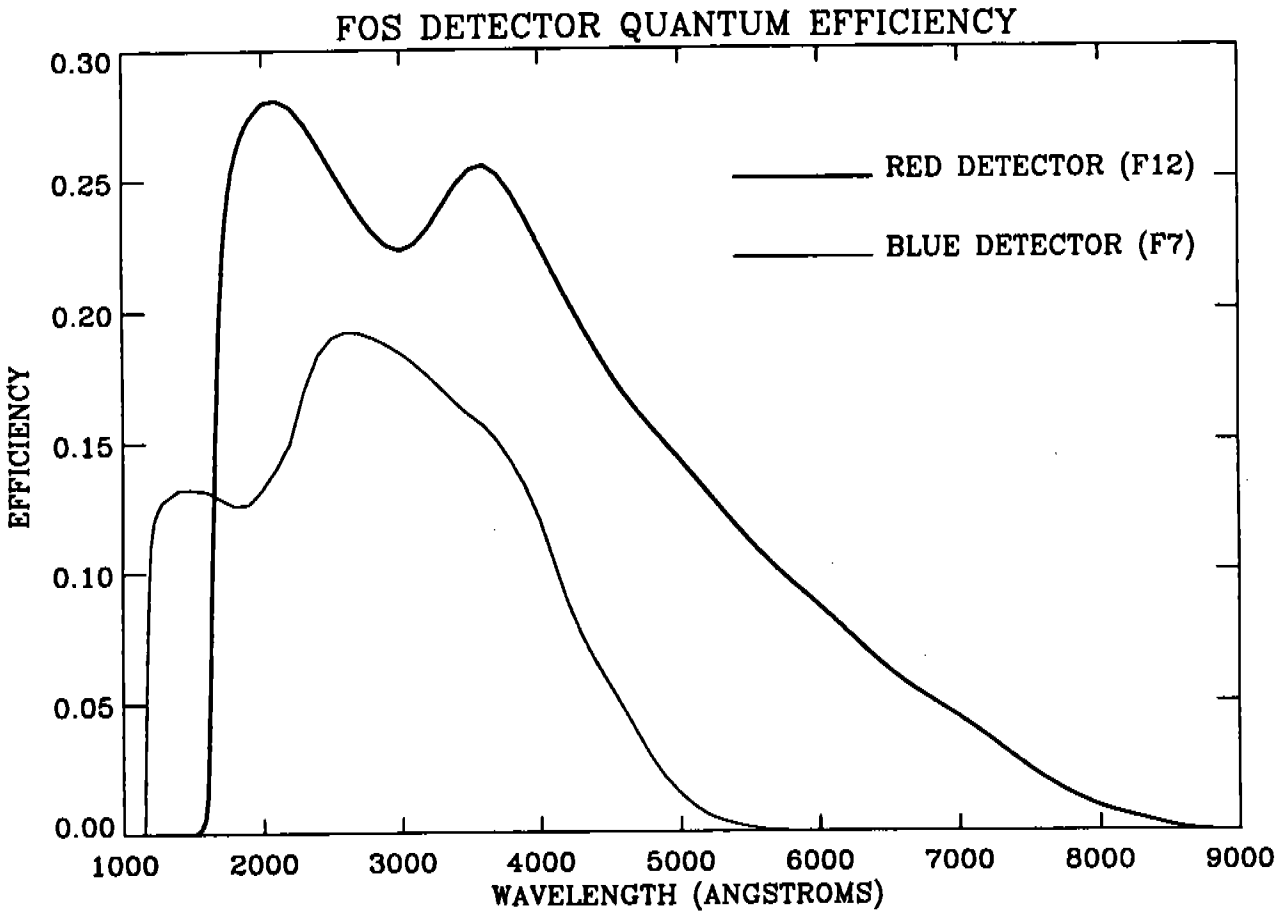

Figure 1.0.1: Quantum efficiency of the FOS Flight detectors.

Gratings are available with both high spectral resolution (1 to 6Å diode^{-1}, $\lambda/\Delta\lambda \approx 1300$) and low spectral resolution (6 to 25Å diode^{-1}, $\lambda/\Delta\lambda \approx 250$). The actual spectral resolution depends on the point spread function of HST, the dispersion of the grating, the aperture used, and whether the target is physically extended.

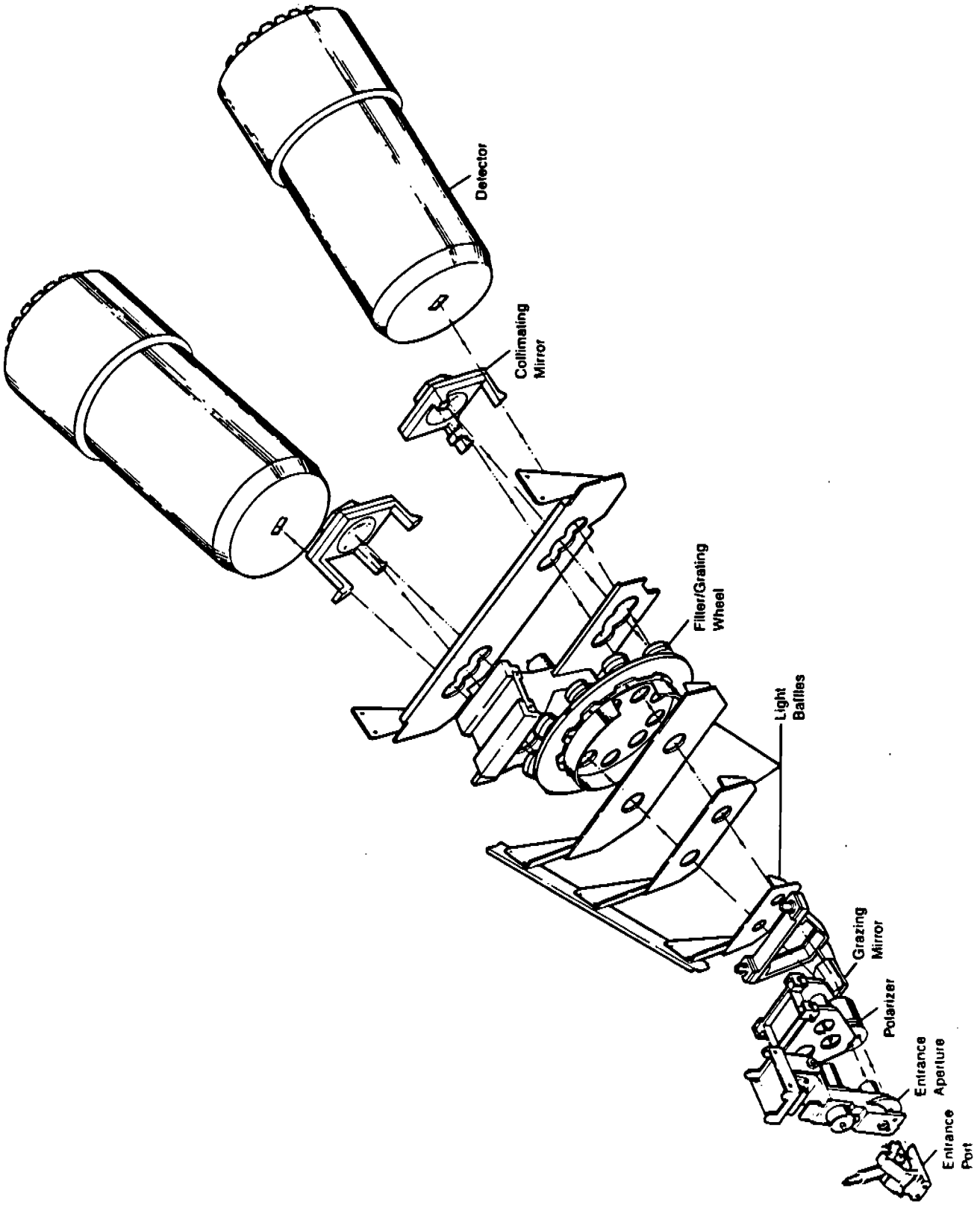

Figure 1.0.2: A schematic optical diagram of the FOS.

The instrument has the ability to take spectra with high time resolution ($\geq$ 0.03 seconds, RAPID mode), and the ability to bin spectra in a periodic fashion (PERIOD mode). Although FOS originally had polarimetric capabilities, polarimetry may be possible only in the G270H grating after the installation of the Corrective Optics (COSTAR) because of the strong instrumental polarization introduced by the two extra reflections.

There is a large aperture for acquiring targets using on-board software ($3.7'' \times 3.7''$, designation 4.3). A variety of science apertures are available; a large aperture for collecting the maximum light (effectively $3.7'' \times 1.2''$, designation 4.3); several circular apertures with sizes $0.86''$ (1.0), $0.43''$ (0.5), and $0.26''$ (0.3); and paired square apertures with sizes $0.86''$ (1.0-PAIR), $0.43''$ (0.5-PAIR), $0.21''$ (0.25-PAIR), and $0.09''$ (0.1-PAIR), for isolating spatially resolved features and for measuring sky.

The effect of the lack of sufficient magnetic shielding on the red detector, originally causing the image on the photocathode to drift as much as the width of a diode, will be corrected on-orbit by adjusting the magnetic field of the detectors according to the position in orbit and according to the direction of pointing. The on-orbit correction is expected to be in place by April of 1993. A similar image drift with excursions of about 1/3 those on the red side will be corrected on-orbit on the blue side at the same time.

The blue side sensitivity has decreased at a rate of about 10% per year from launch until 1992.0 but now appears to be more stable. The red side sensitivity is generally stable to within 5%, but has been observed to decrease rapidly in a highly wavelength dependent fashion between 1800Å and 2100Å, affecting gratings G190H, G160L, and to a lesser degree G270H. Flat fields have been obtained in the large $4.3'' \times 1.4''$ aperture (4.3) for these three gratings every month since January 1992, and will continue to be taken several times a year in both the large aperture and in the slit, so that a library of flat fields is available to assist in the removal of this effect (see Figures in Section 3.). However, the flat fields for these 3 gratings have changed little since early 1992. The sensitivity of both the blue and the red detectors is being monitored approximately every 4 months.

1.1 Spectral Resolution

The spectral resolution depends on the point spread function of the telescope, the dispersion of the grating, the aperture, and whether the target is extended or is a point source. Table 1.1.1 lists the gratings, their wavelengths, and their dispersions (Kriss, Blair, & Davidsen 1991). All available FOS apertures are listed in Table 1.1.2 with their designation as given in HST headers, their size, and their shape. Figure 1.1.1 shows the FOS entrance apertures overlaid upon each other, together with the diode array. The positions of the apertures are accurately known and highly repeatable.

The spectral resolution (FWHM) is given as a function of aperture in Table 1.1.3 in units of diodes for a point source at 3400Å and for a uniform, extended source. The FWHM does not vary strongly as a function of wavelength, so that this FWHM, together with the dispersion of the gratings given in Table 1.1.1, can be used to approximate the effective spectral resolution. For example, observing a point source using the red side with the G270H grating in the $3.7'' \times 1.2''$ aperture (4.3) gives a spectral resolution of

$$\text{FWHM} = 0.96 \text{ diode} \times 2.05\text{Å diode}^{-1},$$

$$\text{FWHM} = 1.97\text{Å}.$$

Table 1.0.1
FOS at a Glance

Wavelength coverage[1]	FOS/BL: 1150Å to 5400Å in several grating settings.
	FOS/RD: 1620Å to 8500Å in several grating settings.
Spectral resolution	High: $\lambda/\Delta\lambda \approx 1300$.
	Low: $\lambda/\Delta\lambda \approx 250$.
Time resolution	$\Delta t \geq 0.03$ seconds.
Acquisition aperture	$3.7'' \times 3.7''$ (4.3)
Science apertures[2]	Largest: $3.7'' \times 1.2''$ (4.3),
	Smallest: $0.09''$ square paired (0.1-PAIR),
Brightest observable stars[3]	$V \approx 8$ for B0V, $V \approx 6$ for G2V.
Dark count rate	FOS/BL: 0.007 counts s^{-1} $diode^{-1}$.
	FOS/RD: 0.01 counts s^{-1} $diode^{-1}$.
Example exposure time[4]	$F_{1300} = 2.5 \times 10^{-13}$, SNR=20/(1.0Å), t=180s
$0.9''$ aperture	$F_{2800} = 1.3 \times 10^{-13}$, SNR=20/(2.0Å), t=5.8s (FOS/BL)
	$F_{2800} = 1.3 \times 10^{-13}$, SNR=20/(2.0Å), t=4.0s (FOS/RD)

GHRS at a Glance

Wavelength coverage, resolution[5]	1050Å to 3400Å $\lambda/\Delta\lambda = 2,500$.
	With ≈ 300Å coverage per grating setting.
Wavelength coverage, resolution	1050Å to 3400Å $\lambda/\Delta\lambda = 25,000$.
	With ≈ 40Å coverage per grating setting.
Wavelength coverage, resolution	1050Å to 3400Å $\lambda/\Delta\lambda = 80,000$.
	With ≈ 10Å coverage per grating setting.
Time resolution	$\Delta t \geq 0.05$ seconds.
Large science aperture (LSA)	$1.74'' \times 1.74''$.
Small science aperture (SSA)	$0.22'' \times 0.22''$.
Brightest acquireable stars	No limit.
Dark count rate	0.01 counts s^{-1} $diode^{-1}$.
Example exposure time (LSA)[6]	$F_{1300} = 2.5 \times 10^{-13}$, SNR=20/(0.065Å), t=2000s
	$F_{2800} = 1.3 \times 10^{-13}$, SNR=20/(0.14Å), t=1000s

[1] See Table 1.1.1 for grating dispersions and wavelength coverage.
[2] See Table 1.1.2 for all available apertures.
[3] See Table 1.3.1 for brightest observable objects, which are strongly dependent on spectral type and grating.
[4] See Section 1.2 for exposure time calculations, and Table 1.2.1 for count rates for objects with a variety of spectral types. The example given here is for 3C273.
[5] See the GHRS Instrument Handbook for details.
[6] The example given here is for 3C273, from Morris *et al.* 1991. For the large science aperture, the small increase in throughput from the improved PSF is approximately the same as the small decrease in throughput due to the extra two reflections of COSTAR.

Table 1.1.1
FOS Dispersers

Grating	Diode No. at Low λ	Low λ (Å)	Diode No. at High λ	High λ (Å)	Δλ (Å-Diode^{-1})	Blocking Filter
			Blue Digicon			
G130H	60	1150[1]	516[7]	1606	1.00	--
G190H	1	1573	516	2330[4]	1.47	--
G270H	1	2222	516	3301	2.09	SiO_2
G400H	1	3240	516	4823	3.07	WG 305
G570H	1	4575	516	6872[3]	4.45	WG 375
G160L	318	1150[1]	516	2510[4]	6.87	--
G650L	295	3540	373	9022[3]	70.28	WG 375
PRISM	175	1850[2]	24	5500[3]	--	--
			Red Digicon*			
G190H	516	1565[5]	1	2312[5]	-1.45	--
G270H	516	2223	1	3278	-2.05	SiO_2
G400H	516	3238	1	4784	-3.00	WG 305
G570H	516	4571	1	6820	-4.37	WG 375
G780H	516	6272	1	9219[6]	-5.72	OG 530
G160L	126	1600[5]	1	2430	-6.64	--
G650L	205	3540	1	8729	-25.44	WG 375
PRISM	332	1850	497	8950[6]	--	--

[1] The blue Digicon's MgF_2 faceplate absorbs light shortward of 1150 Å.
[2] The sapphire prism absorbs light shortward of 1650 Å; however, because of the large dispersion of the prism at the shortest wavelengths, the effective cutoff is longward of 1650 Å.
[3] Quantum efficiency of the blue tube is very low longward of 5500 Å.
[4] The second order overlaps the first order longward of 2300 Å, but its contribution is at a few percent.
[5] The red Digicon's fused silica faceplate strongly absorbs light shortward of 1650 Å.
[6] Quantum efficiency of the red detector is very low longward of 8600 Å.
[7] The photocathode electron image typically is deflected across 5 diodes, effectively adding 4 diodes to the length of the diode array

* Wavelength direction is reversed for the red side relative to the blue side.

Table 1.1.2
FOS Apertures

Designation (Header Designation)	Number	Shape	Size (″)	Separation (″)	Special Purpose
0.3 (B-2)	Single	Round	0.26 dia	NA	Spectroscopy and Spectropolarimetry
0.5 (B-1)	Single	Round	0.43 dia	NA	Spectroscopy and Spectropolarimetry
1.0 (B-3)	Single	Round	0.86 dia	NA	Spectroscopy and Spectropolarimetry
0.1-PAIR (A-4)	Pair	Square	0.09	2.57	Object and Sky
0.25-PAIR (A-3)	Pair	Square	0.21	2.57	Object and Sky
0.5-PAIR (A-2)	Pair	Square	0.43	2.57	Object and Sky
1.0-PAIR (C-1)	Pair	Square	0.86	2.57	Extended Objects
0.25 x 2.0 (C-2)	Single	Rectangular	0.21 x 1.71	NA	High Spectral Resolution
0.7 x 2.0-BAR (C-4)	Single	Rectangular	0.60 x 1.71	NA	Surrounding Nebulosity
2.0-BAR (C-3)	Single	Square	1.71	NA	Surrounding Nebulosity
BLANK (B-4)	NA	NA	NA	NA	Dark and Particle Events
4.3 (A-1)	Single	Square	3.66 x 3.71	NA	Target Acquisition and Spectroscopy
Failsafe	Pair	Square	0.43 and 3.7	NA	Target Acquisition and Spectroscopy

The first dimension of rectangular apertures is along the dispersion direction, and the second dimension is perpendicular to the dispersion direction. The two apertures with the suffix designation "BAR" are bisected by an occulting bar which is 0.26" wide in the direction perpendicular to the dispersion.

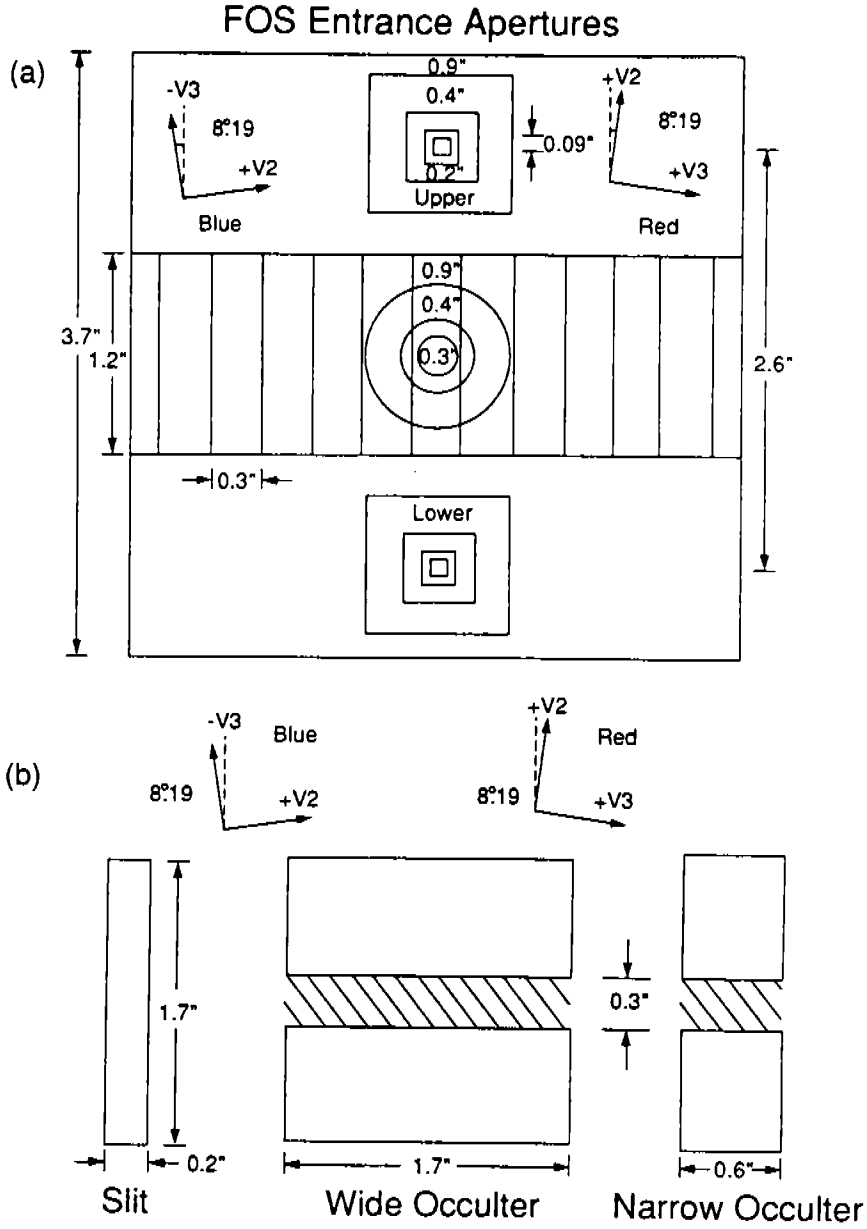

Figure 1.1.1: A Schematic of the FOS Apertures projected onto the sky. The upper panel shows the array of $0.30'' \times 1.23''$ diodes projected across the center of the $3.66'' \times 3.71''$ target acquisition aperture. The target acquisition aperture and the single circular apertures position to a common center. The pairs of square apertures position to common centers with respect to the target acquisition aperture as shown in the figure. Either the upper aperture (the "A" aperture, which is furthest from the HST optical axis) or the lower aperture (the "B" aperture, which is closest to the HST optical axis) in a pair can be selected by an appropriate y-deflection in the Digicon detectors. The lower panel shows the three slits position to the center of the target acquisition aperture. The figure shows the orientation of the direction perpendicular to the dispersion relative to the HST V2, V3 axes. The FOS x-axis is parallel to the diode array and positive to the left; the y-axis is perpendicular to the diode array and positive toward the upper aperture. Note that the angle between the FOS/BLUE and the FOS/RED slit orientation is 73.6 degrees.

Table 1.1.3
FOS Line Widths (FWHM) as a Function of Aperture Size

Designation	Size (″)	Uniform Source		Point Source at 3400Å FWHM
		G130H (Blue) FWHM	G570H (Red) FWHM	
0.3	0.26 (circular)	1.00 ± .01	0.95 ± .02	0.92
0.5	0.43(circular)	1.27 ± .04	1.20 ± .01	0.93
1.0	0.86(circular)	2.29 ± .02	2.23 ± .01	0.96
0.1-PAIR	0.09(square)	0.97 ± .03	0.92 ± .02	0.91
0.25-PAIR	0.21(square)	0.98 ± .01	0.96 ± .01	0.92
0.5-PAIR	0.43(square)	1.30 ± .04	1.34 ± .02	0.94
1.0-PAIR	0.86(square)	2.65 ± .02	2.71 ± .02	0.96
0.25 X 2.0	0.21 X 1.71(slit)	0.99 ± .01	0.96 ± .01	0.92
0.7 X 2.0-BAR	0.60 X 1.71	1.83 ± .02	1.90 ± .01	1.26
2.0-BAR	1.71	5.28 ± .07	5.43 ± .04	1.34
4.3	3.66 X 3.71	12.2 ± 0.1	12.2 ± 0.1	0.96

The FWHM are given in units of diodes. A diode is 0.30″ wide and 1.23″ high.

The same observation with the 0.2″ × 1.7″ (`0.25X2.0`) slit would have a spectral resolution of

$$\text{FWHM} = 0.92 \text{ diode} \times 2.05\text{Å diode}^{-1},$$

$$\text{FWHM} = 1.89\text{Å}.$$

The line spread functions computed from a model point spread function at 2250Å through the FOS apertures are shown in Figure 1.1.2 in units of microns, where 1 diode width = 50 microns.

1.2 Exposure Time Calculations

The information necessary to calculate exposure time is given here in several forms. First, the HST + FOS + COSTAR efficiencies (Figure 1.2.1), aperture throughputs (Figure 1.2.2), and wavelength dispersions (Table 1.1.1), are given together with a series of relations between count rate and input spectra (Table 1.2.1). Then, count rate per diode at the wavelength corresponding approximately to the peak sensitivity of the given grating is provided in tabular form for a number of spectral types for objects with V=15 (Table 1.2.2). Finally, the count rate per diode is shown in Figure 1.2.3 for both detectors and all gratings,

FOS Line Spread Function at 2250Å

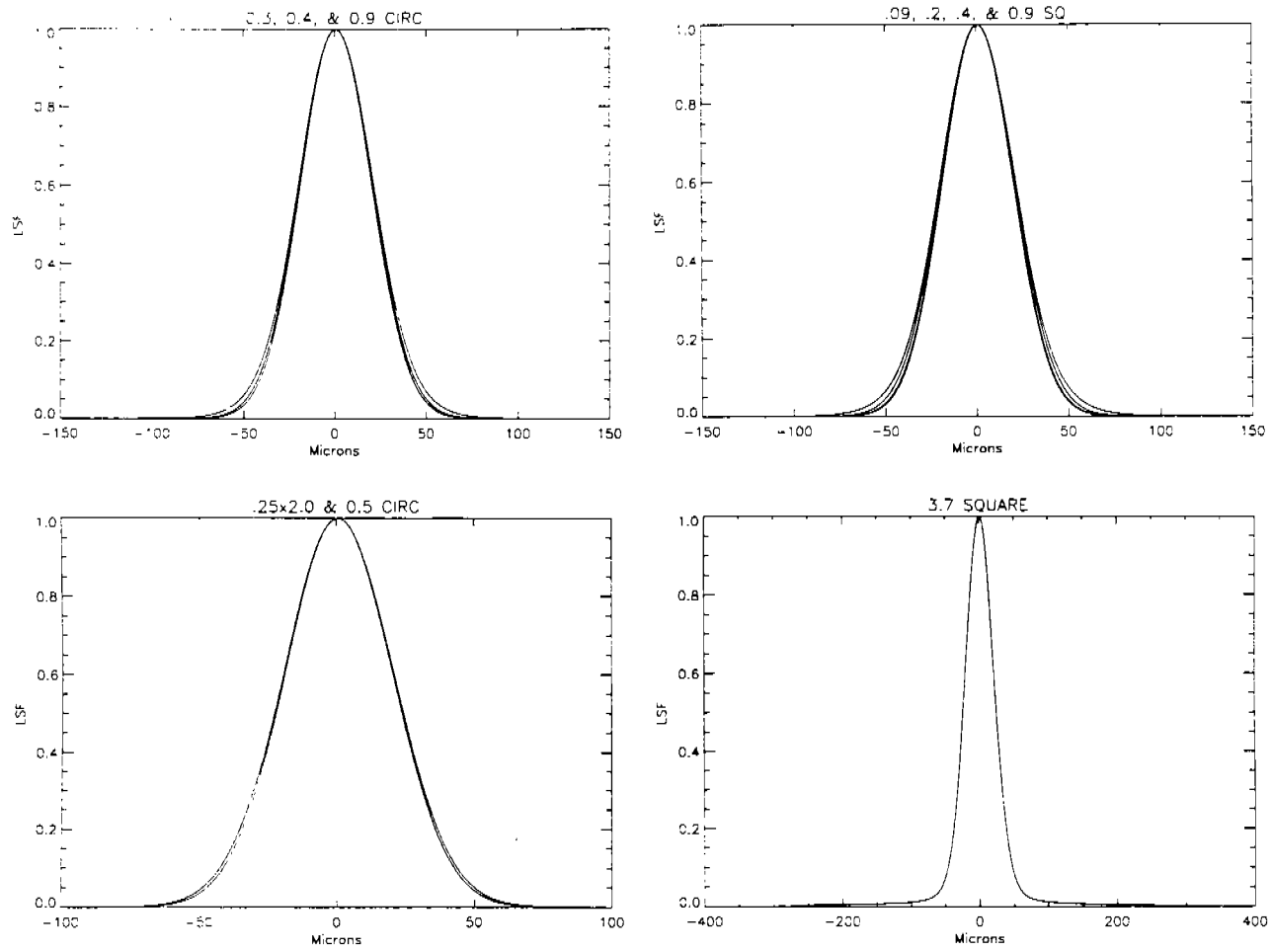

Figure 1.1.2: The solid curves are spectral line spread functions for various FOS apertures. Ordinate shows relative intensity versus distance in the dispersion direction in microns (one diode, equal to one nominal spectral resolution element, is 50 microns).

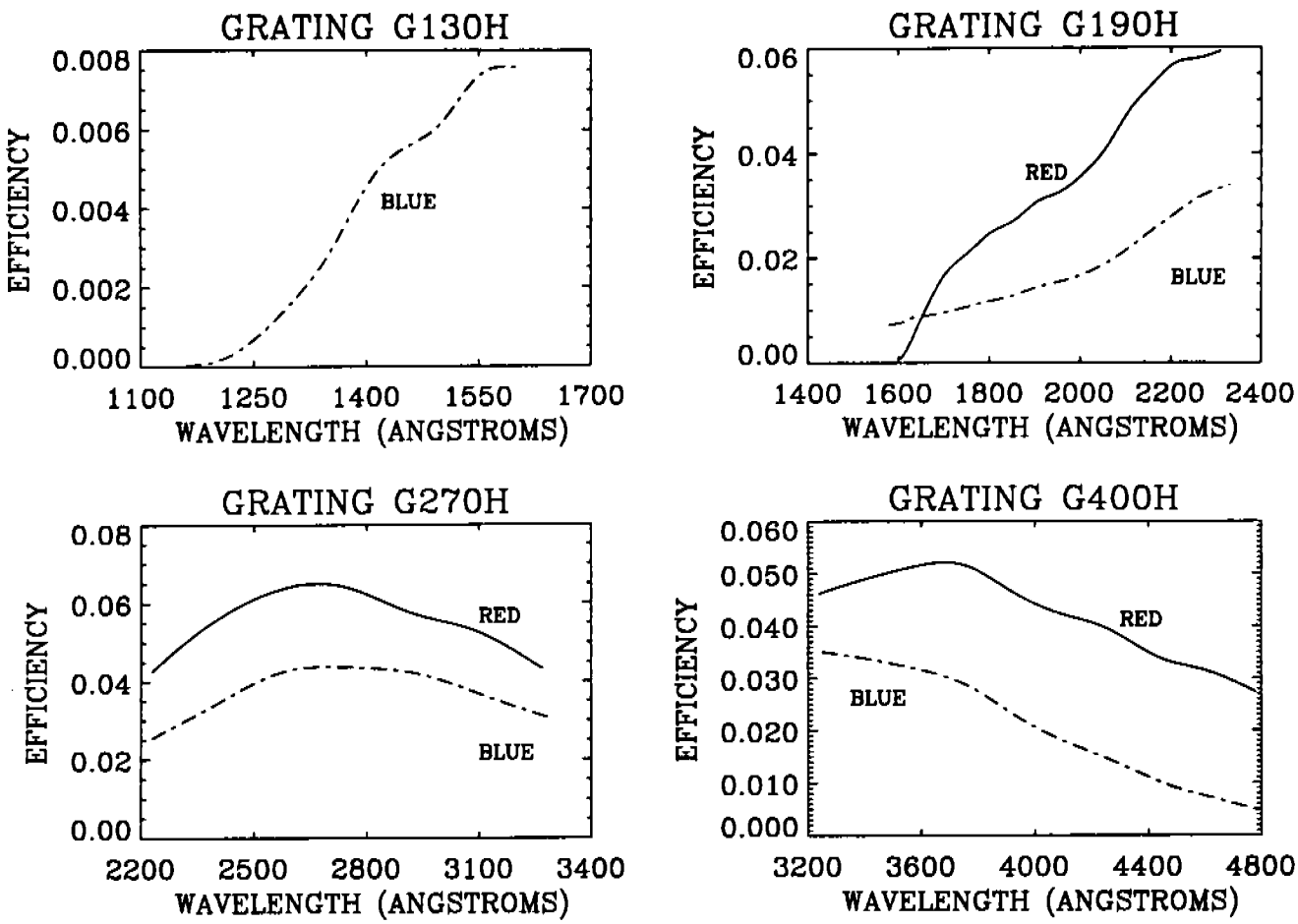

Figure 1.2.1: HST + FOS + COSTAR Efficiency, E_λ vs. λ.

assuming a flat input spectrum ($F_\lambda \propto \lambda^0 = 1.4 \times 10^{-14}$ erg cm^{-2} s^{-1} Å^{-1}) observed in the 0.9″ aperture (1.0).

For example, the count rate for a point source with flux of $F_\lambda = 3.5 \times 10^{-15}$ erg cm^{-2} s^{-1} Å^{-1} at 3700Å using the red detector, in the 0.9″ aperture (1.0), with the G400H grating, is given by equation 1 in Table 1.2.1,

$$N_\lambda = 2.28 \times 10^{12} F_\lambda (\lambda \Delta\lambda) E_\lambda T_\lambda.$$

where $F_\lambda = 3.5 \times 10^{-15}$ erg cm^{-2} s^{-1}, $\lambda = 3700$Å, $\Delta\lambda = 3.0$Å (from Table 1.1.1), the efficiency is $E_\lambda = 0.052$ (from Figure 1.2.1), and the throughput is $T_\lambda = 0.95$ (from Figure 1.2.2), so that

$$N_\lambda = 4.4 \text{ counts s}^{-1}\text{diode}^{-1}.$$

The exposure time for a desired signal-to-noise ratio per resolution element is then given by $t = SNR^2$ counts diode^{-1}/N_λ counts sec^{-1} diode^{-1}, which for $SNR = 20$ (for example), gives $t = 400/4.4$ counts sec^{-1} diode^{-1} = 91 s.

As a comparison, count rates for objects of representative spectral type with V=15.0 are given in Table 1.2.2 at the wavelengths corresponding to the peak response of a given

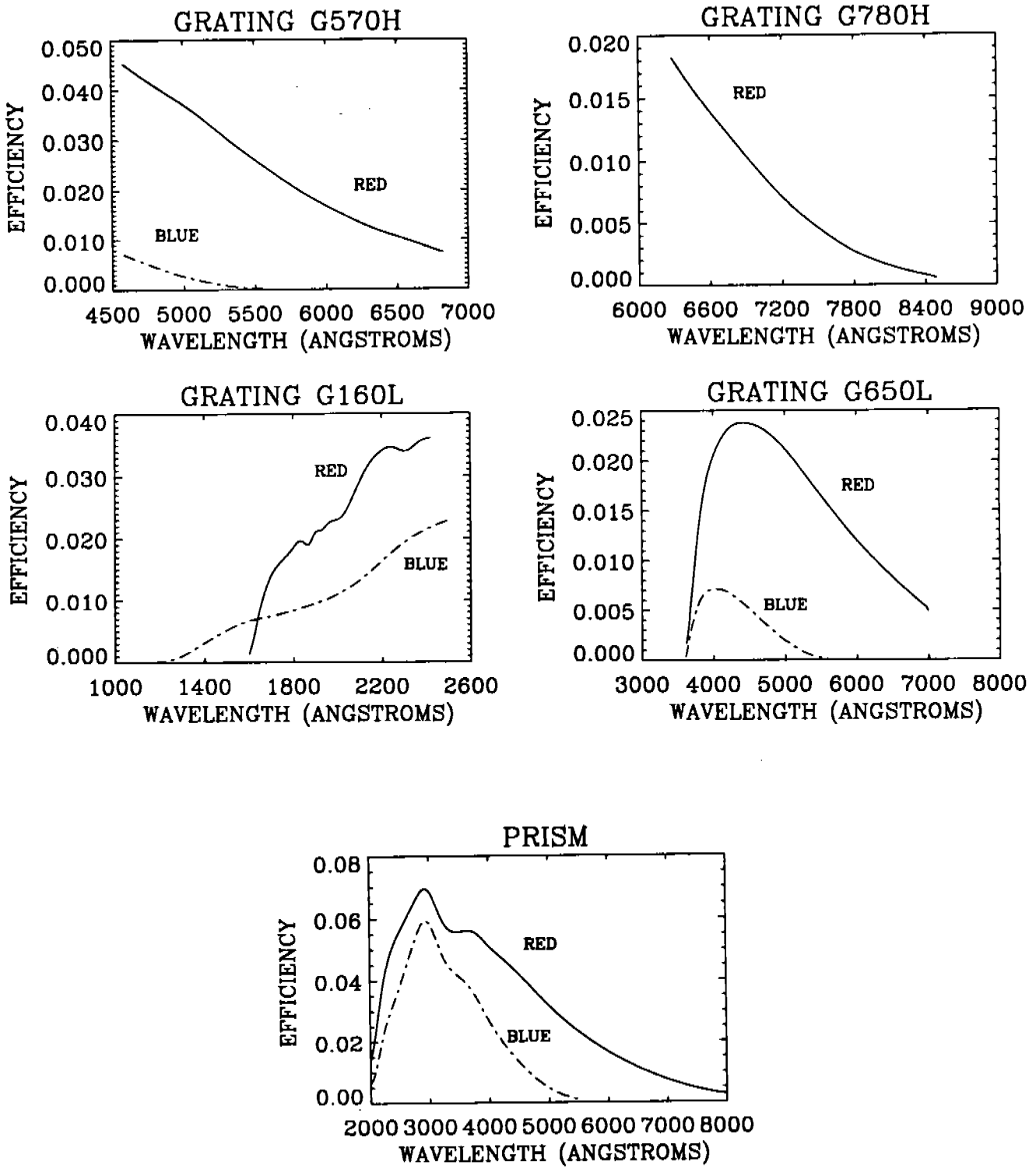

Figure 1.2.1 (cont.): HST + FOS + COSTAR Efficiency, E_λ vs. λ.

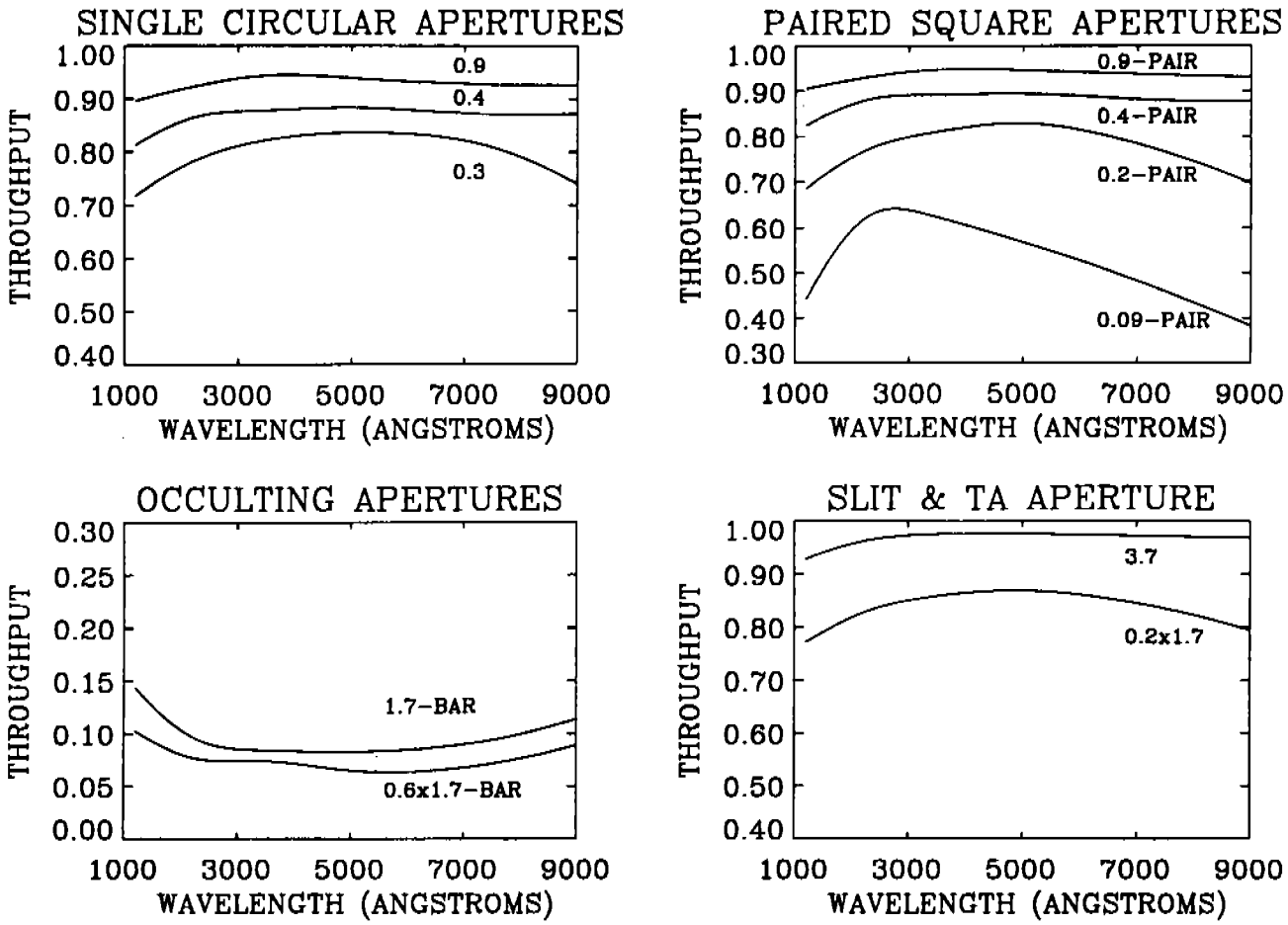

Figure 1.2.2: Fraction of light transmitted by the apertures after deployment of COSTAR for a perfectly centered point source.

grating. The example given above corresponds to an object with power law $F_\nu \propto \nu^{-2}$, V=15.0, observed with the G400H grating on the red side.

Alternatively, the count rate for observations in the 0.9″ (1.0) aperture can be read directly from Figure 1.2.3 and scaled to the appropriate flux. For the example given above, with $F_\lambda = 3.5 \times 10^{-15}$erg cm^{-2}s^{-1}Å^{-1}, the count rate per diode at 3700 Å is given by $N_\lambda = (3.5 \times 10^{-15}/1.0 \times 10^{-14}) \times n$ counts sec^{-1} diode^{-1}, $= 0.35 \times 12.0 = 4.2$ counts s^{-1} diode^{-1}. To calculate the count rate in other science apertures, the count rate must be corrected according to the relative throughputs in Figure 1.2.2.

When observing in time resolved modes, the total observing time can become dominated by the read-out time for FOS data. Section 1.4 below discusses the time to read-out the FOS in the context of RAPID observations.

1.3 Brightness Limits

The Digicon detectors can be damaged if illuminated by sources that are too bright. The brightness limits of the detectors have been translated into a limit of total counts detected in 512 diodes per 60 seconds—the overlight limit. If the overlight limit is exceeded in a 60 second interval, the FOS automatically safes—*i.e.*, the FOS shuts its aperture door, places all

Ian says this doesn't take into account the obscuration from the secondary

Table 1.2.1

FOS Observed Counts Sec-1 Diode-1 (Nl) for Points Sources at Wavelength l (Å)

Flux Distribution	Inputs	Equation for Nl (counts- sec-1 diode-1)
1. Continuum	Fl(ergs cm-2 s-1 Å-1)	16% too high $2.28 \times 1012\, F_\lambda D_\lambda E_\lambda T_\lambda$
2. Monochromatic	Il(ergs cm-2 s-1)	$2.28 \times 1012\, I_\lambda E_\lambda T_\lambda$
3. Normalized Continuum	$\frac{F_\lambda}{F_{5556}}, m_{5556}$	$7720 \frac{F_\lambda}{F_{5556}} \lambda \Delta\lambda E_\lambda T_\lambda 10^{-0.4 m_{5556}}$
4. Planck Function	Teff(K), m5556	$1.09 \times 10^{22} \left(\frac{e^{\frac{25897}{T}} - 1}{e^{\frac{1.4388 \times 10^8}{\lambda T}} - 1} \right) \Delta\lambda \frac{E_\lambda T_\lambda 10^{-0.4 m_{5556}}}{\lambda^4}$
5. Continuum	Fl(ergs cm-2 s-1 hz-1)	$6.83 \times 10^{30} \frac{F_v \Delta\lambda E_\lambda T_\lambda}{\lambda}$
6. Normalized Continuum	$\frac{F_v}{F_{v,5556}}, m_{5556}$	$2.38 \times 10^{11} \frac{F_v}{F_{v,5556}} \frac{\Delta\lambda E_\lambda T_\lambda}{\lambda} 10^{-0.4 m_{5556}}$
7. Power Law n-a	a, m5556	$2.38 \times 10^{11} \left(\frac{\lambda}{5556}\right)^{\alpha} \left(\frac{\Delta\lambda E_\lambda T_\lambda}{\lambda}\right) 10^{-0.4 m_{5556}}$

E_λ = (Net HST Reflectivity) x (FOS Efficiency at Wavelength l (Å)) x (COSTAR efficiency). See Figure 1.1.3.
T_λ = Throughput of aperture at Wavelength l (Å) as simulated based on Telescope Image Modelling software (Burrows and Hasan 1991). See Figure 1.1.4.
D_λ = Number of Angstroms per diode at Wavelength l (Å). See Table 1.1.1.

Note that the relevant count rate to derive SNR per resolution element is Nl (counts- sec-1 diode-1). A resolution element is one diode, regardless of sub-stepping.

Table 1.2.2
Simulated counts-sec^{-1}-diode^{-1} for unreddened objects in the 0.9″ (**1.0**) aperture at 15th magnitude.

Blue Detector								
Spectral Type	G130H (λ_{peak}=1600 Å)	G190H (λ_{peak}=2300 Å)	G270H (λ_{peak}=2650 Å)	G400H (λ_{peak}=3250 Å)	G570H (λ_{peak}=4600 Å)	G160L (λ_{peak}=2440 Å)	G650L (λ_{peak}=4000 Å)	PRISM (λ_{peak}=4000 Å)
B0V	3.0	11	19	17	2.4	33	20	2.4×10^2
A5V	-	0.44	1.1	2.2	1.7	1.4	11	1.0×10^2
G2V	-	-	0.17	1.3	1.3	0.12	5.7	53
ν^{-1}	0.28	1.8	3.8	4.8	1.4	6.2	8.2	87
ν^{-2}	0.08	0.79	1.9	2.9	1.2	2.7	5.9	61
Red Detector								
Disperser (λ_{peak})	G190H (λ_{peak}=2300 Å)	G270H (λ_{peak}=2650 Å)	G400H (λ_{peak}=3600 Å)	G570H (λ_{peak}=4600 Å)	G780H (λ_{peak}=6300 Å)	G160L (λ_{peak}=2400 Å)	G650L (λ_{peak}=4400 Å)	PRISM (λ_{peak}=4000 Å)
B0V	22	29	19	14	2.9	56	49	3.6×10^2
A5V	0.84	1.7	3.2	10	3.3	1.9	30	2.0×10^2
G2V	-	0.24	2.2	7.9	4.3	0.15	22	1.1×10^2
ν^{-1}	3.5	5.5	6.6	8.4	4.7	10	25	1.6×10^2
ν^{-2}	1.5	2.7	4.3	7.0	5.2	4.5	20	1.2×10^2

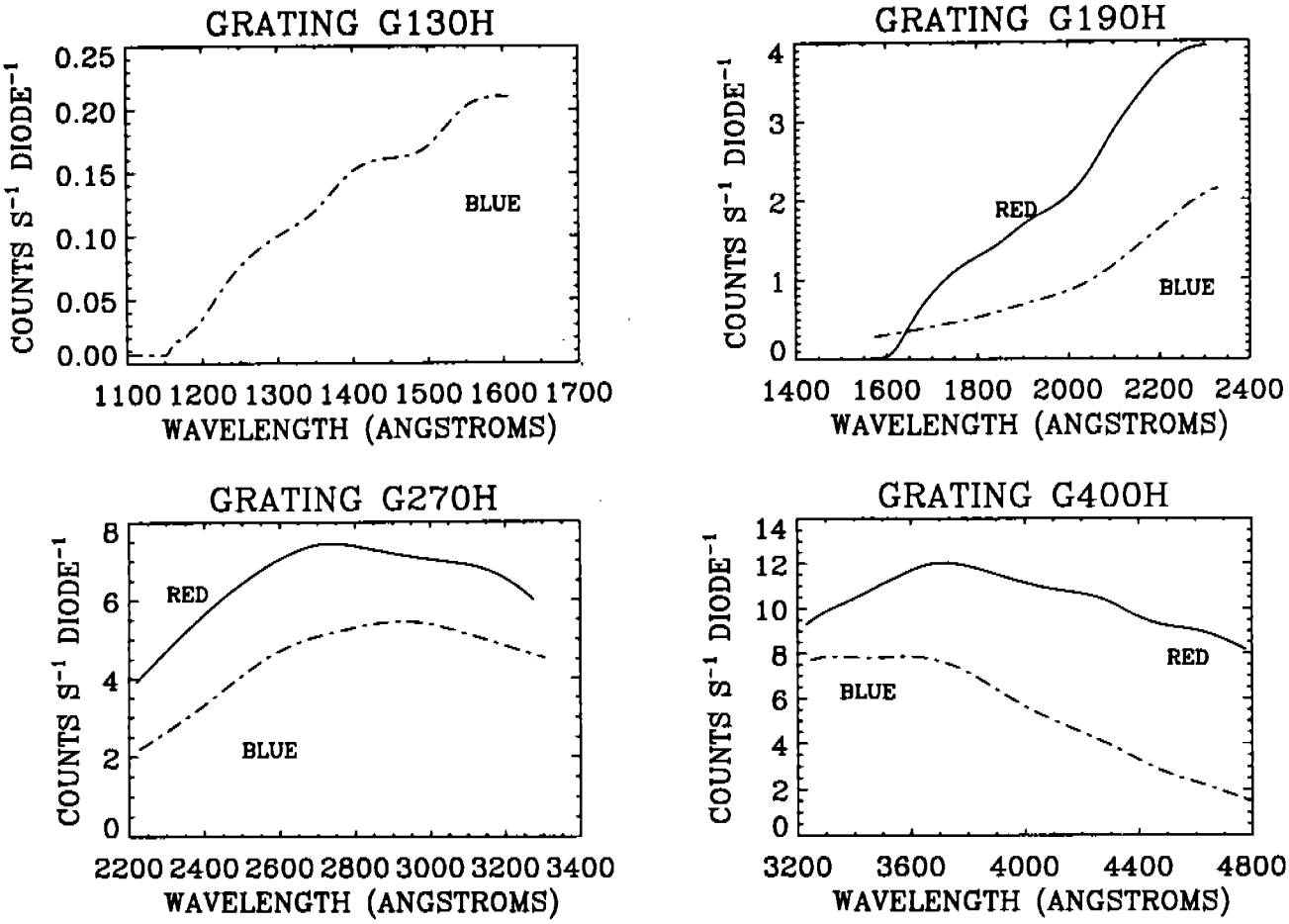

Figure 1.2.3: Simulation of detected counts-s^{-1}-diode^{-1} for the post-COSTAR FOS 0.9″ (**1.0**) aperture. Input spectrum is $F_\lambda = 1 \times 10^{-14}$ erg-cm^{-2}-s^{-1}-Å^{-1} ($F_v \propto V^{-2}$; V = 13.9).

wheels at their rest position, and stops operation. The overlight protection limit is 1.2×10^8 counts per minute summed over the 512 diodes for the gratings and 3×10^6 counts per minute for the mirror. The visual magnitudes for unreddened stars of representative spectral types corresponding to this limiting count rate are given in Table 1.3.1 for all grating settings. The restrictions on target brightness are also found in the Bright Object Constraints Table of the Proposal Instructions (Table 5.15).

1.4 Time Resolution

The manner that FOS data are taken depends on which of the three modes (ACCUM, RAPID, or PERIOD) are used.

FOS data are taken in a nested manner, with the innermost loop being livetime plus deadtime (see Appendix A for a full description of data taking). The next loop is taken by sub–stepping the diode array along the dispersion direction (X direction), with steps one-quarter of the diode width (12.5 micron, or 0.076″). To minimize the impact of dead diodes, the next loop of data–taking is performed by sub–stepping in steps of one-quarter of the diode width, but starting at the adjacent diode. This over–scanning is repeated until spectra are taken starting at 5 continuous diodes.

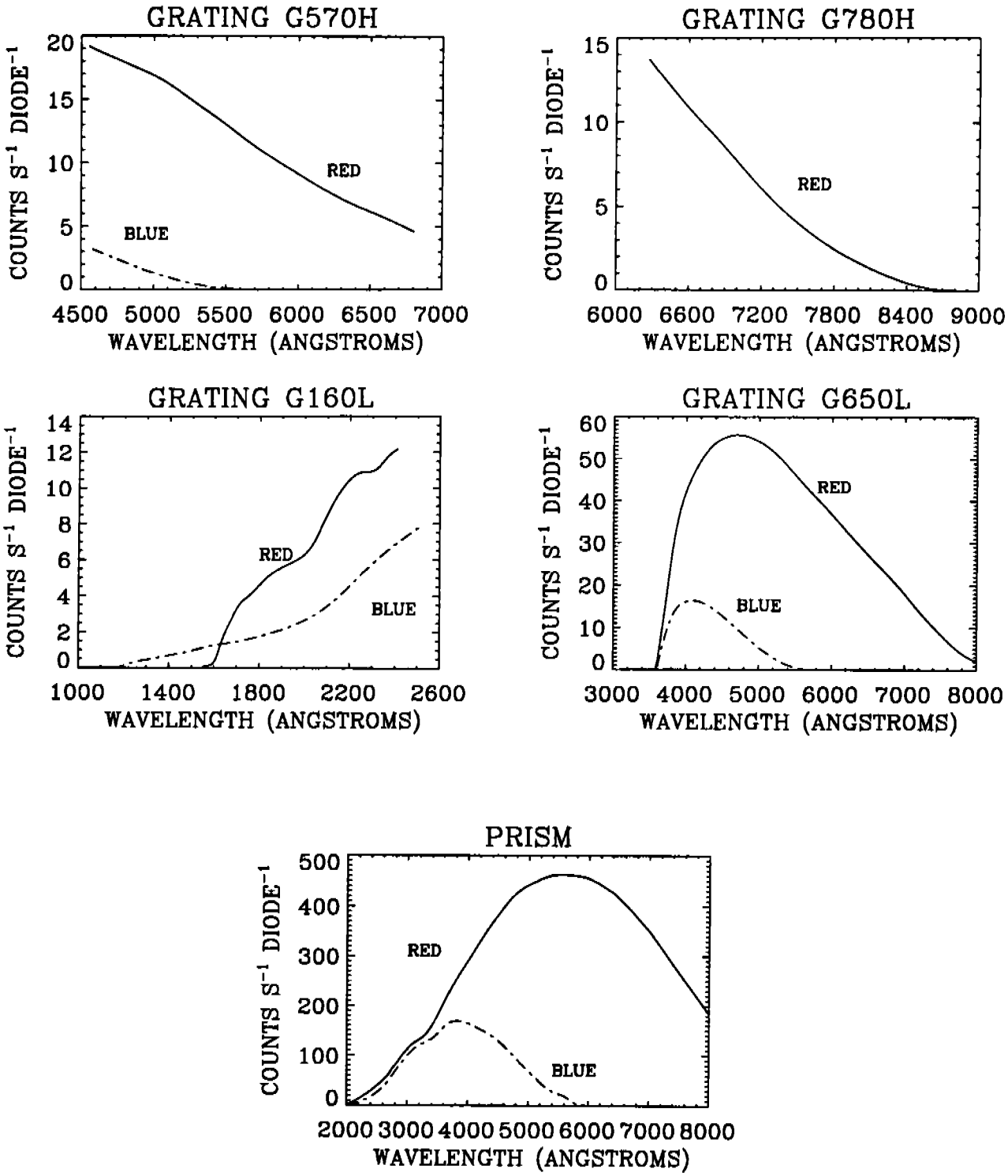

Figure 1.2.3 (cont.): Simulation of detected counts-s^{-1}-diode^{-1} for the post-COSTAR FOS 0.9″ (**1.0**) aperture. Input spectrum is $F_\lambda = 1 \times 10^{-14}$ erg-cm^{-2}-s^{-1}-Å^{-1} ($F_V \propto V^{-2}$; V = 13.9).

Table 1.3.1
Brightness Limits

Spectral Type	$B-V$	Red Side Brightness Limits								
		G190H	G270H	G400H	G570H	G780H	G160L	G650L	PRISM	MIRROR
07V	−0.32	9.3	9.8	9.0	7.9	5.7	10.3	8.2	10.5	14.8
B0V	−0.30	9.1	9.5	9.0	7.9	5.6	10.1	8.1	10.3	14.6
B1.5V	−0.25	8.8	9.4	8.8	7.9	5.7	10.0	8.1	10.2	14.5
B3V	−0.20	8.1	8.7	8.6	7.9	5.7	9.5	8.1	9.8	14.0
B6V	−0.15	7.9	8.6	8.4	7.8	5.7	9.3	8.0	9.6	13.8
B8V	−0.11	7.1	7.9	8.4	7.8	5.7	9.0	8.0	9.3	13.5
A1V	+0.01	5.9	7.0	8.0	7.8	5.8	8.6	7.9	8.9	13.1
A2V	+0.05	5.7	6.8	8.0	7.8	5.8	8.5	7.9	8.8	13.0
A6V	+0.17	5.1	6.5	7.9	7.8	5.8	8.4	7.8	8.7	12.9
A7V	+0.20	5.0	6.4	7.8	7.8	5.9	8.3	7.8	8.7	12.8
A9V	+0.28	4.4	6.2	7.7	7.8	6.0	8.2	7.7	8.6	12.7
F0V	+0.30	4.2	6.1	7.7	7.7	6.0	8.2	7.7	8.5	12.7
F5V	+0.44	3.6	6.1	7.5	7.7	6.1	8.1	7.6	8.5	12.6
F7V	+0.48	2.9	5.6	7.4	7.7	6.1	8.0	7.6	8.3	12.5
F8V	+0.52	2.7	5.4	7.3	7.7	6.1	8.0	7.6	8.3	12.5
G2V	+0.63	2.1	5.3	7.3	7.7	6.2	7.9	7.6	8.3	12.4
G6V	+0.70	—	5.2	7.2	7.7	6.2	7.9	7.5	8.2	12.4
K0V	+0.81	—	4.3	7.0	7.7	6.2	7.8	7.5	8.1	12.3
K0III	+1.00	—	3.4	6.6	7.6	6.3	7.7	7.5	8.0	12.2
K5V	+1.15	—	3.5	6.3	7.6	6.4	7.6	7.4	7.9	12.1
K4III	+1.39	—	2.1	6.0	7.5	6.5	7.5	7.3	7.8	12.0
M2I	+1.71	—	—	5.5	7.4	6.5	7.3	7.2	7.6	11.8
$\alpha = 1$		6.9	7.9	8.0	7.8	6.4	8.8	7.8	9.1	13.3
$\alpha = 2$		5.8	7.1	7.6	7.7	6.7	8.4	7.7	8.8	12.9
$\alpha = -2$	−0.46	10.2	10.3	9.2	8.0	5.8	10.9	8.2	10.8	15.4
$T = 50{,}000°$		9.6	9.9	9.0	7.9	5.7	10.4	8.2	10.5	14.9

A typical data taking sequence would divide the exposure time into twenty equal bins, and then perform the sequence of (livetime + deadtime), stepped four times. That sequence would be performed 5 times, each time stepping to the next diode. As each of the 5 over–scanned spectra are obtained, they are added to the same memory locations of the previous spectra, so that the over–scanning does not increase the amount of data. The data taking is then performed as (livetime + deadtime) × sub–stepping × over–scanning, or

$$(\mathrm{LT} + \mathrm{DT}) \times 4 \times 5.$$

1.4.1 ACCUM

FOS observations longer than a few minutes are time resolved. Spectra taken in a standard manner in ACCUM mode are read out at regular intervals. The red side (FOS/RD) is read out at $\leq$ 2 minute intervals, while the blue side (FOS/BL) is read out at $\leq$ 4 minute intervals. The standard output data for ACCUM mode preserve the time resolution in "multi–

Table 1.3.1. *Continued.*

Spectral Type	Blue Side Brightness Limits								
	G130H	G190H	G270H	G400H	G570H	G160L	G650L	PRISM	MIRROR
07V	7.2	8.5	9.3	8.4	5.0	9.8	6.5	10.0	14.3
B0V	7.0	8.3	9.1	8.3	5.0	9.7	6.4	9.8	14.2
B1.5V	6.6	8.0	9.0	8.2	4.9	9.5	6.3	9.7	14.0
B3V	5.8	7.3	8.3	7.9	4.9	8.9	6.3	9.2	13.4
B6V	5.4	7.1	8.2	7.7	4.9	8.7	6.1	9.0	13.2
B8V	4.5	6.2	7.5	7.6	4.9	8.2	6.2	8.6	12.7
A1V	2.3	5.1	6.5	7.2	4.8	7.5	6.0	8.0	12.0
A2V	—	4.8	6.4	7.2	4.8	7.4	6.0	7.9	11.9
A6V	—	4.2	6.1	7.1	4.7	7.2	5.8	7.8	11.7
A7V	—	4.2	6.1	7.0	4.7	7.2	5.8	7.7	11.7
A9V	—	3.5	5.9	6.9	4.7	7.1	5.7	7.6	11.6
F0V	—	3.4	5.8	6.8	4.6	7.0	5.6	7.5	11.5
F5V	—	2.9	5.7	6.7	4.6	6.9	5.5	7.4	11.4
F7V	—	—	5.3	6.6	4.5	6.7	5.4	7.2	11.2
F8V	—	—	5.1	6.5	4.5	6.6	5.3	7.1	11.1
G2V	—	—	5.0	6.5	4.5	6.5	5.3	7.1	11.0
G6V	—	—	4.9	6.3	4.4	6.4	5.2	7.0	10.9
K0V	—	—	4.1	6.1	4.4	6.1	5.1	6.7	10.6
K0III	—	—	3.1	5.7	4.3	5.7	4.8	6.3	10.2
K5V	—	—	3.2	5.3	4.2	5.4	4.6	6.0	9.9
K4III	—	—	—	4.9	4.0	5.0	4.3	5.6	9.5
M2I	—	—	—	4.4	3.8	4.6	4.0	5.2	9.1
$\alpha = 1$	4.2	6.1	7.5	7.3	4.6	8.0	5.7	8.4	12.5
$\alpha = 2$	2.8	5.0	6.7	6.9	4.5	7.4	5.4	7.9	11.9
$\alpha = -2$	8.6	9.4	9.8	8.6	5.0	10.6	6.6	10.4	15.1
$T = 50{,}000°$	7.5	8.8	9.4	8.4	5.0	10.0	6.4	10.0	14.5

(see section # of Our Book)

group" format. Each group of data is preceded by group parameters with information that can be used to calculate start time of the interval, plus a spectrum for each 2 minute (4 minute) interval of the observation. Each consecutive spectrum (group) is made up of the sum of all previous intervals of data. The last group of the data set contains the spectrum from the full exposure time of the observation.

1.4.2 RAPID

For objects needing higher time resolution, RAPID mode reads out FOS data at a rate set by the observer with the parameter READ-TIME. The shortest READ-TIME is 0.036 seconds. RAPID data is also in group format but contains a header only at the beginning of the data. Each group then contains group parameters with FOS related information followed by the spectrum for one time segment. (Of particular interest among the group parameters is FPKTTIME, which is used to derive the start time for each individual exposure, as given in Appendix A.)

READ-TIME is equal to livetime plus deadtime plus the time to read out FOS,

$$\text{READTIME} = (\text{LT} + \text{DT}) \times \text{INTS} \times \text{NXSTEPS} \times \text{OVERSCAN} \times \text{YSTEPS} \times \text{SLICE} \times \text{NPATT} + \text{Readout time.}$$

The read-out time for FOS is dependent on the telemetry rate, and on the amount of data to be read out, which is dependent on number of diodes (*i.e.*, the wavelength range) being observed, as well as on the sub-stepping. For the fastest **READ-TIMES**, the rate of reading data can be stepped up from the default telemetry rate of 32kHz to 1MHz, the wavelength region can be decreased, and sub-stepping set to 1. (The data size, which cannot exceed 12,288 pixels, is given by

$$\text{Data size} = (\text{NCHNLS} + \text{MUL} - 1) \times \text{SUBSTEP} + \text{MUL} \times \text{SUBSTEP}$$

where **NCHNLS** is the number of diodes read out, **MUL** is the multiplicity, or the number of diodes that are over-scanned (usually 5), and **SUBSTEP** is the number of steps along the dispersion (usually 4). The relation between number of diodes read out and wavelength coverage can be derived from Table 1.1.1. (Table 1.1.1 is accurate to within a few Ångstroms since it is based on data that was not corrected for the geomagnetically induced image drift, Kriss, Blair, & Davidsen (1991). See also Section 3.1 on wavelength calibrations.)

For a standard **ACCUM** exposure, the data size, which cannot exceed 12,288 units, is given by

$$\text{Data size} = (512 + \text{MUL} - 1) \times \text{SUBSTEP} + \text{MUL} \times \text{SUBSTEP}$$

$$\text{Data size} = (512 + 4) \times 4 + 5 \times 4 \text{ !!}$$

$$\text{Data size} = 2,064. \quad = 2084 \text{ !!}$$

The read out time for spectral data is given by

$$\text{Readout time} = 0.0335 \times \text{INT}\left(\frac{\text{Data size}}{N}\right)$$

where INT(Data size/N) is the next largest integer corresponding to the ratio of Data size divided by 50 for the first packet, and divided by 61 for all subsequent packets. This equation is for data that is read out at the 32kHz data rate. If more than 20% of **READ-TIME** is spent reading out data, then the faster data rate is used, so that the read out time becomes

$$\text{Readout time} = 0.0028 \times \text{INT}\left(\frac{\text{Data size}}{N}\right)$$

When the faster data rate is in use, there is a limit of twenty minutes to the amount of contiguous data that can be recorded, due to the storage capacity of the onboard tape recorder.

1.4.3 PERIOD

For objects that have a well known period, FOS data can be taken in **PERIOD** mode in such a way that the period is divided into **BINS**, where each bin has a duration of Δt = period/**BINS**. The period of the object is specified by the parameter **CYCLE-TIME**. The spectrum taken during the first segment of the period, Δt_1, is added into the first memory location. The spectrum taken during the second segment, Δt_2, is added to a contiguous memory location, and so

on. The number of segments that a period can be divided into depends on the amount of data each spectrum contains, which depends on the number of sub-steps, whether or not the data are overscanned, and how large a wavelength region is to be read out. If the full range of diodes are read out, and the default observing parameters are used, 5 **BINS** of data can be stored. **PERIOD** mode data are single group, with a standard header followed by the spectra stored sequentially, where there are **BINS** spectra.

The data size, which cannot exceed 12,288 pixels, is given for **PERIOD** by

$$\text{Data size} = (\text{NCHNLS} + \text{MUL} - 1) \times \text{SUBSTEP} \times \text{BINS}$$

where **BINS** applies to **PERIOD** mode only. **BINS** is the number of time–segments into which the periodic data are divided. If the observer needs a larger number of **BINS** than 5, the wavelength range can be decreased, or the sub–stepping can be decreased to 2 or 1. (See Table 1.1.1 for relation between number of diodes [NCHNLS], and wavelength dispersion.)

1.5 Polarization

The deployment of COSTAR will result in two extra reflections for light entering the FOS. These extra reflections introduce instrumental polarization so that polarization measurements will become difficult and possibly unfeasible with the FOS. However, the section on polarization is included here because the FOS team felt that the G270H grating may be used for polarization observations if it can be properly recalibrated.

A Wollaston prism plus rotating waveplate can be introduced into the FOS to produce twin dispersed images of the slit in opposite senses of polarization at the detector (Allen and Angel 1982). Although there are two waveplates available, only waveplate B is currently recommended for use, and only in the G270H grating. (See Allen and Smith 1992 for polarization calibration results.)

Although the "A" waveplate was designed to do well at Lyα λ 1216Å, the split spectra are not well separated by the "A" waveplate, so that the polarization at Lyα cannot be observed. Linear polarization observations should use the "B" waveplate and gratings G130H, G190H, and G270H.

The sensitivity of the polarizer depends upon its throughput efficiency. The detector can only observe one of the two spectra produced by the polarizer so that another factor of two loss in practical throughput occurs. The count rate is given by

$$\text{Count rate(pol)} = \text{Count rate(FOS)} \times \eta_{thr} \times 0.5,$$

where η_{thr} is found in Figure 1.5.1.

1.6 FOS Noise and Dynamic Range

The minimum detectable source levels are set by instrumental background, while the maximum accurately measurable source levels are determined by the response times of the FOS electronics.

When the FOS is operating outside of the South Atlantic Anomaly, the average dark count rate is roughly 0.01 counts s^{-1} $diode^{-1}$ for the red detector and 0.007 counts s^{-1} $diode^{-1}$ for the blue detector (Rosenblatt *et al.* 1992). However, Rosenblatt *et al.* note that the background count rate varies with geomagnetic latitude so that higher rates are observed at higher latitudes. The detected counts s^{-1} $diode^{-1}$ plots given in Figure 1.2.3 for an input

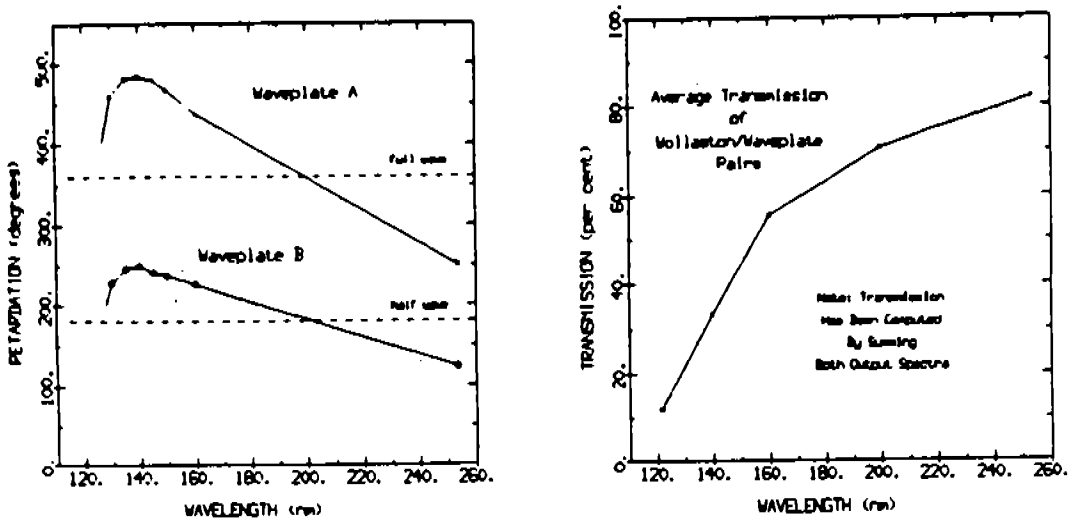

Figure 1.5.1: FOS waveplate retardation (left) and polarimeter transmission (Allen & Angel, 1982).

spectrum with constant flux of $F_\lambda = 1 \times 10^{-14}$ erg cm^{-2} s^{-1} Å^{-1} can be compared with the observed dark count rate to determine the limiting magnitude for the FOS. For example, for an object observed at 2600Å with the red side in the 0.9″ (1.0) aperture, an incident flux of $F_\lambda = 1.4 \times 10^{-17}$ erg cm^{-2} s^{-1} Å^{-1} would produce a count rate comparable to the red side dark rate. For an object observed at 2600Å with the blue side in the 0.9″ (1.0) aperture, an incident flux of $F_\lambda = 1.4 \times 10^{-17}$ erg cm^{-2} s^{-1} Å^{-1} would produce a count rate comparable to the blue side dark rate.

In the other extreme, for incident count rates higher than approximately 100,000 counts s^{-1} diode^{-1}, the observed output count rate does not have an accurate relation with the true input count rate. Figure 1.6.1 shows a determination of the relation between true count rate and observed count rate, as measured by Lindler and Bohlin (1986, measured for high count rates for the red side only). For observed count rates above 50,000 counts s^{-1} diode^{-1}, the correction exceeds a factor of 2 and the accuracy decreases drastically. By the time a true count rate of 200,000 counts s^{-1} diode^{-1} is reached, the error in the correction to the true rate is of order 50%.

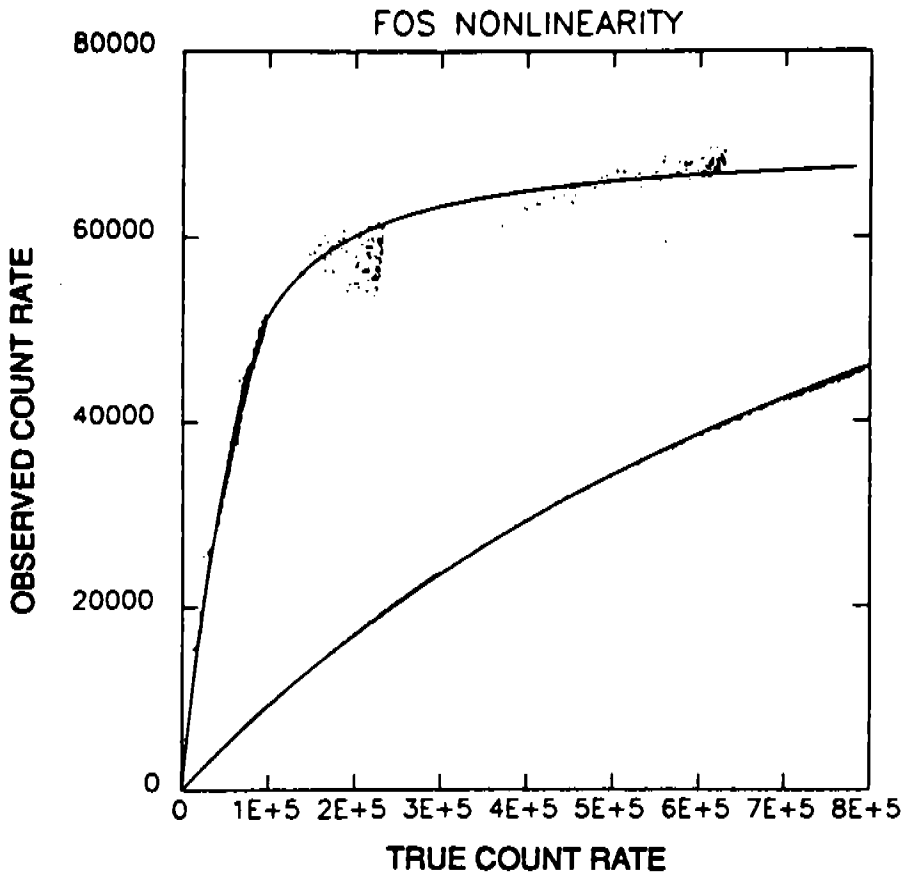

Figure 1.6.1: Measured count rate versus true count rate (D. Lindler and R. Bohlin, 1986). The lower curve is a plot of the upper curve expanded by 10 in the x-direction.

2. OBSERVING MODES

2.1 Acquiring the Target

The HST pointing is accurate and reliable. To demonstrate the accuracy of the HST pointing achieved after guide star acquisition, Figure 2.1.0 shows the slews performed to center the target in the science aperture after FOS target acquisition, for observations taken after early 1991. The position $V_2 = 0.0$ and $V_3 = 0.0$ in Figure 2.1.0 corresponds to perfect initial pointing. Figure 2.1.0 shows that, using positions derived from GASP, about 70% of the blind pointings fall within $1''$ of the aperture center. However, an onboard target acquisition is still necessary with the FOS to center the target in the science aperture.

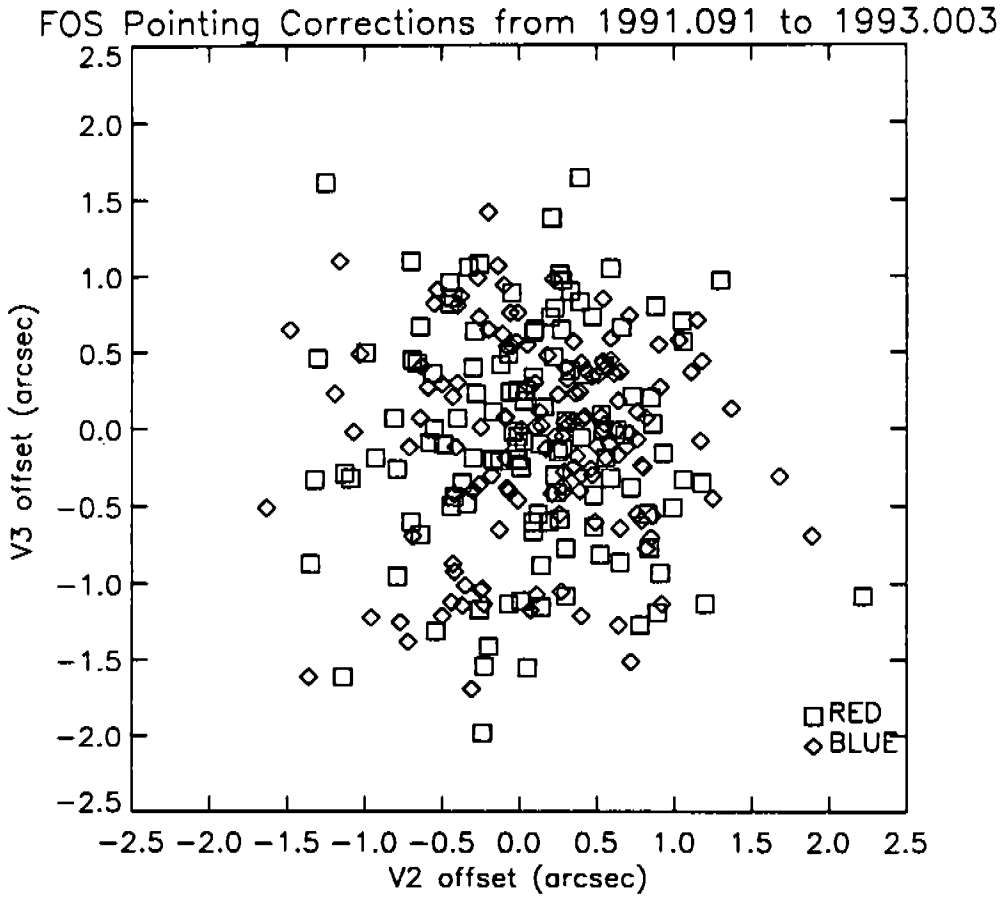

Figure 2.1.0: Slews performed after FOS target acquisition (after guide star acquisition) to center the target in the science aperture. The average red side offset, based on 128 acquisitions, is: V2 = $0.08'' \pm 0.05''$, V3 = $-0.05'' \pm 0.06''$. The average blue side offset, based on 148 acquisitions, is: V2 = $0.15'' \pm 0.05''$, V3 = $-0.06'' \pm 0.05''$. Seventy percent of the pointings after guide star acquisitions are within $1''$ of the target.

An interactive acquisition (set with the `SPECIAL REQUIREMENT INT ACQ`) and three onboard acquisition modes (`ACQ/BINARY`, `ACQ/PEAK`, and `ACQ/FIRMWARE`) are described below. During an onboard acquisition, the telescope slews to the object, performs the acquisition, calculates the small offset required to center the target in a science aperture, makes the offset, and then begins the science exposure. In contrast, during an interactive acquisition there must be a

real time contact with HST, and the observer must be present at the ST ScI to interpret the image. Because of the probability of confusion when looking at an FOS white light picture, we believe that in nearly all cases a WFPC2 assisted target acquisition will be a better scientific choice than an FOS acquisition (ACQ). However, ACQ does also provide an important means of verifying, after the fact, where the FOS aperture was positioned on the target during a science exposure, for both WFPC2 early acquisition and for onboard acquisitions of targets in complex fields.

The FOS acquisition aperture is $3.7'' \times 3.7''$ square (4.3). In order to have a 95% chance of placing a star in this aperture, the star *must* have an RMS positional error with respect to the guide stars of less than $1.0''$. The FOS finds the star by deflecting its electronic image along the diode array and perpendicular to the diode array. The acquisition aperture is 12 diodes wide and 3 diodes high, as illustrated in Figure 1.1.1. Because the diode is rectangular, with the X direction smaller than the Y direction ($0.31'' \times 1.23''$), the two directions are treated differently in target acquisition.

Additional acquisitions are not necessary when switching from the red side to the blue side for the $0.9''$ (1.0) or larger apertures, since the aperture positions are accurately known. Once a target has been acquired into a large science and observed with one detector, a slew can be performed to place the target directly into the aperture for the other detector. Such "side-switch" slews would not be accurate enough to place objects in the $0.2'' \times 1.2''$ slit (0.25X2.0) or the $0.3''$ aperture (0.3), however. In these cases and additional ACQ/PEAK) is required as summarized in Table 2.1 (see also section 2.1.3 and examples in Appendix F).

Table 2.1
Typical FOS Acquisition Sequences

Acquisitions starting with ACQ/BINARY

Science Aperture	First Acq	Second Acq	Dimension X x Y	Acquisition Aperture
4.3	ACQ/BINARY	–		
1.0	ACQ/BINARY	–		
0.5	ACQ/BINARY	ACQ/PEAK	3X3	0.5
0.3	ACQ/BINARY	ACQ/PEAK	4X4	0.3
SLIT	ACQ/BINARY	ACQ/PEAK	~~1X7~~	SLIT

Acquisitions using only ACQ/PEAK

Science Aperture	First Acq	Second Acq	Third Acq	Fourth Acq
4.3	3X1 with 4.3	2X6 with 1.0	–	–
1.0	3X1 with 4.3	2X6 with 1.0	3X3 with 0.5	–
0.5	3X1 with 4.3	2X6 with 1.0	3X3 with 0.5	4X4 with 0.3
0.3	3X1 with 4.3	2X6 with 1.0	4X4 with 0.3	5X5 with 0.3
SLIT	3X1 with 4.3	2X6 with 1.0	3X3 with 0.5	~~1X7~~ with SLIT

Side-switching will be allowed ONLY for those objects where the total RPSS spacecraft time (both sides combined) is less than 6 hours. ST ScI reserves the right to change the order of the sides (and gratings) to most efficiently schedule the observation.

Three rules apply to any side-switching specification:

1. Specify the target acquisition (TA) exposures on the Exposure Logsheet for one side, while in a comment specifying the parameters such as exposure time, **FAINT**, **BRIGHT**, and spectral element for the other side of FOS. Such a specification will allow easy change of order of the detectors. If the proposer feels the TA must be performed with a specific detector, this must be stated in the General Form, question 5.
2. The special requirement **GROUP NO GAP** should be used in the Exposure Logsheet to link all exposures of the target.
3. If the proposer has a *scientific* need to obtain the observations in a specific grating order, the special requirement **SEQ NO GAP** should be used.

See the Exposure Logsheet lines 3.0 through 4.3 (Appendix F) for an example of a side-switching specification.

~~2.1.1~~ INT ACQ

The mode **ACQ**, when used with the **SPECIAL REQUIREMENT**, **INT ACQ FOR**, maps the acquisition aperture and sends the image to the ground in real time. The apparent elongation of stars in the y-direction caused by the shape of the diodes ($0.21'' \times 1.23''$) is removed on the ground by multiplying the picture by an appropriate matrix. After the picture has been restored, the astronomer measures the position of the target on the image. The small offset required to move the target to the center of one of the science apertures is calculated and uplinked to the telescope; after the slew is performed the science observations begin.

A modified form of interactive acquisition, the dispersed–light interactive acquisition utilizing **IMAGE** mode, may be employed for acquisition of sources in which spectral features of known wavelength are prominent. This method has proven quite useful for planetary satellite acquisitions. Spacecraft overheads for this procedure are no different than the overheads for conventional **INT/ACQ**.

ACQ can also be used after another type of acquisition to provide a picture which shows where HST is pointed in FOS detector coordinates. The Exposure Logsheets provide an example (lines 5–8) of an **ACQ/BINARY** of an offset star followed by an offset onto the nucleus of M81. In this example, after the science observation is made, a (white light) picture of the aperture is taken by using **ACQ** to verify the aperture position.

2.1.2 ACQ/BINARY

ACQ/BINARY is the method of choice for targets with well known energy distributions, but *should not be used for variable sources, sources of unknown color, or extended sources.* The method has a restricted dynamic range of brightness. Specifically, target brightness uncertainty should be less than 0.5 magnitudes for the use of **ACQ/BINARY**. Objects of poorly known color should be acquired with **ACQ/PEAK**.

During an **ACQ/BINARY**, the camera mirror reimages the FOS focal plane onto the Digicon. Acquisition of the target is performed not by moving the telescope, but by deflecting the image of the target acquisition aperture on the photocathode until the target has been placed on the Y edge of the diode. **ACQ/BINARY** first finds the number of stars in the $3.7'' \times 3.7''$ acquisition aperture (designation **4.3**) by integrating at three different positions in the Y-

direction. The program locates the target in one of the three strips, measures its count rate, and locates the target in the X direction. The algorithm then positions the target on the Y–edge of the diode array by deflecting the image across the diode array through a geometrically decreasing sequence of Y–deflections until the observed count rate from the star is half that when the object is fully positioned on the diode array. **ACQ/BINARY** is the preferred acquisition mode for point sources.

Although **ACQ/BINARY** is designed to obtain the Nth brightest star in a crowded field by setting the optional parameter **NTHSTAR**, acquisitions in crowded fields have not been attempted.

There should be about 300 counts in the peak pixel for each y-step that is on-target for Binary Search to succeed. If the number of counts in the peak is significantly larger than 300, the tolerances for when the target is half in the aperture become very small since they are based on $\sqrt{N}$ statistics. Typical centering error after Binary Search is $\lesssim 0.2''$.

A target must lie within the range of counts specified by the Optional Parameters **BRIGHT** and **FAINT**. We recommend that **BRIGHT** and **FAINT** be set to allow for targets 10 times brighter and 5 times fainter than expected. Since the maximum number of y-steps in Binary Search is 11, the default values for the parameters are **BRIGHT** = 300 × 11 × 10 = 33,000 and **FAINT** = 300 × 11/5 = 660.

An Example of an **ACQ/BINARY** on an offset star followed by an FOS observation of the target star is given on lines 1 and 2 of the sample Logsheets.

2.1.2 ACQ/PEAK

During **ACQ/PEAK** the telescope slews and integrates at a series of positions on the sky with a science aperture in place. At the end of the slew sequence the telescope is returned to the position with the most counts. In the case of an **ACQ/PEAK** into a barred aperture, or when using the Optional Parameter **TYPE=DOWN**, the telescope is returned to the position with the fewest counts. **ACQ/PEAK** is a relatively inefficient procedure because a minimum of ~ 42 seconds per dwell is required for the telescope to perform the required small angle maneuvers.

This mode is used for objects too bright to acquire with the camera mirror in place, for objects too variable to acquire with **ACQ/BINARY**, to center targets in the smallest apertures, and to position bright point sources on the bars of the occulting apertures in order to observe any surrounding nebulosity. Examples of **ACQ/PEAK** are given on lines 10.3 though 13.3 of the sample Exposure Logsheets. Table 2.1 summarized typical **ACQ/PEAK** sequences.

To acquire objects into the smallest FOS apertures ($0.3''$ (**0.3**), $0.2''$ (**0.25-PAIR**), $0.09''$ (**0.1-PAIR**), and $0.2''$X $1.7''$ slit (**0.25 X 2.0**)), first use a normal **ACQ/BINARY** acquisition, followed by an **ACQ/PEAK** into the science aperture (see Table 2.1). The **ACQ/PEAK** must have a high number of counts to place the target in the center of these smallest apertures ($\approx$ 10000) and spacing between dwells of order $D/5$, where D is the diameter of the Peak Up aperture. See Table 2.1.2 below for exposure times. An example is given in Logsheet lines 3 through 4.1 below.

Note that count rates must not exceed the safety limits for the mirror or the grating selected (see Table 1.3.1 and Table 2.1.1).

The **ACQ/PEAK** mode is also used for acquiring objects that are too bright to observe with the camera mirror in place. For such bright object acquisitions, the science grating is put in

place before the acquisition. The peak-ups for bright objects do not require the high number of counts needed for acquisition into a small aperture. The non-critical **ACQ/PEAK** requires shorter exposure time and spacing between dwells of order $D/2$.

An N by M pattern can be specified by setting **SEARCH-SIZE-X**, **SEARCH-SIZE-Y**, and **SCAN-STEP-X**, **SCAN-STEP-Y**. Examples are given in the Exposure Logsheets lines 10.3 through 13.3

2.1.4 ACQ/FIRMWARE

ACQ/FIRMWARE is an engineering mode that maps the camera-mirror image of the aperture in X and Y with small, selectable Y increments. The FOS microprocessor filters the aperture map and then finds the y-positions of the peaks by fitting triangles through the data. Firmware is less efficient than Binary Search, and fails if more than one object is found within the range of counts set by the observer (**BRIGHT** and **FAINT**).

2.1.5 Early Acquisition Using WFPC2

We recommend using WFPC2 assisted target acquisition when there will be more than two stars in the $3.7''$ (**4.3**) acquisition aperture or when there will be intensity variations across the acquisition aperture which are larger than a few percent of the mean background intensity. A WFPC2 field is taken several months in advance of the science observation. The positions of the target and an offset star are measured in the image and then (at least 2 months later) the positions are updated on the Exposure Logsheet, and the offset star is acquired with **ACQ/BINARY** and finally the FOS aperture is offset onto the target. Although the position of the target can be measured very accurately in the WFPC2 image, the offset star is needed because there is only about a 30% chance that the same guide stars will be in the Fine Guidance Sensors (FGS) when the subsequent FOS observations are made. With new guide stars, the 1σ uncertainty in any position is $0.3''$. Uncertainty in position of the telescope when slewing by $1'$ due to the spacecraft roll is of order $0.05''$. The Wide Field Camera II is made up of three chips of size $1.25'$ on a side. (Note that offsets larger than $30''$ should be discussed with the User Support Branch.)

The first step in a WFPC2 assisted target acquisition is to use a **SPECIAL REQUIREMENT** on the Exposure Logsheets to specify the exposure as an **EARLY ACQ** which must be taken at least two months before the FOS observations (see lines 5 though 8 on the exposure logsheet). The camera, exposure time, filter, and centering of the target in the image should be chosen such that the picture will show both the target and an isolated (no other star within $5''$) offset star which is brighter than $m_V = 20$ and more than 1 magnitude brighter than the background (magnitudes per square arcsecond). In order to insure that an appropriate offset star will be in the WFPC2 image, the centering of the target in the WFPC2 field should be chosen by measuring a plate or CCD image. The Target List for the FOS exposures should provide the offset star with nominal coordinates and with position given as **TBD-EARLY**. (See example lines 4 and 5 on the Target List.) The Target List also should list the position of the offset star as **RA-OFF**, **DEC-OFF**, and **FROM** the target. Alternatively, the offsets can be given as **XI-OFF** and **ETA-OFF**, or **R**, **PA**, see the Phase II Proposal Instructions Section 5.1.4.3 on Positional Offsets.

After the WFPC2 exposure has been taken and the data have been received, the next step is to get the picture onto an image display so you can i), choose an offset star, ii) measure its right ascension and declination, and iii) measure the right ascension and declination of the target relative to the offset star. An STSDAS task (stsdas.wfpc.metric) is available currently

to extract pointing and roll angle information from the WFPC header and to convert WFPC pixels to right ascension and declination. Upon calibration, the task "metric" will also be available for WFPC2. If this program is not available, you will need to patch your WFPC2 image into the Guide Star Catalog reference frame. Based on your choice of an offset star, the ST ScI will choose a pair of guide stars for the FOS observations which will stay in the "pickles" during the move from the offset star to the target. The probability that a suitable pair of guide stars can be found increases as the separation of the offset star and the target decreases. So, choose the offset star as close as possible to the target (but not so close as to violate the background rule in the preceding paragraph). The final step is to send the position of the offset star and the positional offsets to the ST ScI to update the proposal information for your succeeding FOS observations.

2.1.6 Examples

The following section gives examples for acquiring different types of astronomical objects based on the strengths and weaknesses of the various target acquisition methods.

Example: Single Stars

Stars with visual magnitudes brighter than about 12^{th} are too bright for FOS acquisitions with the camera mirror, and observations of objects that bright will safe the instrument. The exact limit depends on the spectral type of the star and on the detector as shown in Table 2.1.1 below. For a list containing many more spectral types, see Table 1.3.1.

Table 2.1.1
FOS Visual Magnitude Limits with Camera Mirror

	O7V	B0V	B3V	A1V	A6V	G2V	K0III	ν^{-1}	ν^{-2}
Red Side Limit	14.8	14.6	14.0	13.1	12.9	12.4	12.2	13.3	12.9
Blue Side Limit	14.3	14.2	13.4	12.0	11.7	11.0	10.2	12.5	11.9

Stars that are too bright for **ACQ/BINARY** can be acquired by using **ACQ/PEAK** with one of the high dispersion gratings instead of the camera mirror (see lines 10.3 though 10.6 on the Exposure Logsheets). If the visual magnitude of a single star or point source is fainter than limits given in Table 2.1.1 above, if the star does not vary by more than 0.5 magnitudes, and if the colors are known, use **ACQ/BINARY** for the acquisition.

Example: Stars Projected on Bright Backgrounds

ACQ/BINARY can successfully find a star projected on a uniform background provided the target acquisition integration time is long enough to give $\sim$ 300 peak counts from the star and the star is at least a magnitude brighter than the background surface brightness in magnitudes per square arcsecond. If star magnitude and the background magnitude differ by less than 1 magnitude, the star can still be acquired with **ACQ/BINARY** by increasing the integration time. Alternatively, the acquisition can be accomplished by using an early acquisition with WFPC2, followed two months later by an FOS acquisition and blind offset.

A different problem arises when the background varies across the acquisition aperture. Because the logic in the **ACQ/BINARY** program drives the star to the edge of the diode array by finding the position which gives half the maximum number of counts, any change in the background in the y-direction will bias the derived y-position of the star. Simulations of acquisitions of stars projected onto bright galaxies such as NGC 3379 show that the shot noise in the star will determine the accuracy (rather than the spatially-variable background), provided the star is at least 15″ from the center of the galaxy.

Example 9 Diffuse Sources and Complex Fields

The FOS onboard acquisition methods were designed to acquire point sources. Consequently, diffuse sources and complex fields must be observed by first acquiring a star and then offsetting to the desired position in the source. The most accurate positioning of the FOS aperture on the source will be accomplished by using a WFPC2 assisted target acquisition. In many programs, the interesting positions in the source will be chosen on the basis of WFPC2 images. If the imaging program is planned as described in the section on WFPC2 assisted TAs, the science images can be used for the acquisition.

Example 10 Nebulosity Around Bright Point Sources

The optimal FOS aperture position for a bright point source surrounded by a nebulosity will depend on the distribution and brightness of the nebulosity relative to the point source. If high spatial resolution images show that the nebulosity has a scale length of a few tenths of an arcsecond and is relatively symmetrical around the source, then the signal-to-noise ratio may be maximized by placing the stellar source on the occulting bar of one of the occulting apertures and simultaneously observing the nebulosity on both sides of the occulting bar. When using this approach, you should first use Binary Search to position the source near the center of the occulting aperture. The second step is to use a Peak Down in the y-direction to position the stellar source on the occulting bar. An example is given in lines 11, 12, and 13 of the Exposure Logsheet.

If high resolution images show that the nebulosity is rather asymmetrical, the best approach may be to observe the nebulosity with one of the small circular apertures. In that case the bright stellar source should be acquired with **ACQ/BINARY**, followed by an **ACQ/PEAK**, followed by an offset onto the nebulosity.

Example 11: ACQ/PEAK

ACQ/PEAK is now the method of choice for targets with variability of order 0.5 magnitudes.. This method utilizes a spatial scan series of exposures to locate the target. The position with the maximum signal is chosen; no positional interpolation is performed. This method must also be used for targets brighter than about V=13 (see Table 1.3.1).

For a planetary object, an area of sky larger than the TA aperture (3.7″ × 3.7″, **4.3**) may have to be searched, plus the object may be too bright to acquire with **ACQ/BINARY**. By using the target acquisition aperture, an effective aperture of size 3.7″ × 1.2″ (designation **4.3**) is available and an area of 7.4″ × 7.4″ can be searched. The first two steps of the **ACQ/PEAK** are to perform a 2 × 6 dwell pattern with the (effective) 3.7″ × 1.2″ aperture (**4.3**). Then the **ACQ/PEAK** sequence outlined in Table 2.1 for the appropriate aperture can be used.

The most time efficient way to acquire a bright target with the FOS is to use the $3.7'' \times 1.2''$ (4.3) aperture in a 1 × 3 dwell pattern, followed by a 6 × 2 dwell pattern into a $0.9''$ (1.0) aperture. The third step depends on the science to be done. As with the example given above, for an object to be centered into the $0.9''$ (1.0) aperture, a non-critical ACQ/PEAK can be performed into the $0.4''$ (0.5) aperture. These types of acquisitions are shown on lines 10.3 through 13.3 on the Exposure Logsheet and summarized in Table 2.1.

2.1.7 Acquisition Exposure Times

There should be about 300 counts in the peak of the y-step that is centered on the star in an ACQ/BINARY exposure. The maximum number of y-steps which can be taken during ACQ/BINARY is 11. Table 2.1.2 summarizes the total exposure time for an ACQ/BINARY, *i.e.* the time per y-step multiplied by 11, for various types of stars. *The exposure times in Table 2.1.2, scaled to the magnitude of the target, are the times that should be entered in the Exposure Logsheets.* There is a minimum integration time that can be entered on the Exposure Logsheet. The minimum is constrained by the FOS livetime limit given in Table 2.1.3. If the exposure time must be larger than that calculated from Table 2.1.2 to accommodate the minimum time, the values for the optional parameters BRIGHT and FAINT must be set to reflect the total number of counts expected.

$$\text{BRIGHT} = 33,000 \times \frac{\text{TIME}_{\text{Table 2.1.3}}}{\text{TIME}_{\text{Table 2.1.2}}}$$

$$\text{FAINT} = 660 \times \frac{\text{TIME}_{\text{Table 2.1.3}}}{\text{TIME}_{\text{Table 2.1.2}}}$$

For example, for a red side ACQ/BINARY of a 12^{th} magnitude offset K0III star, 0.29s is the exposure time derived from Table 2.1.2, but the minimum exposure time is 0.66s. The default values of BRIGHT and FAINT must then be multiplied by the factor 0.66/0.29 = 2.28, so that BRIGHT = 75,100 and FAINT = 1500.

The peak-up exposure times in Table 2.1.2 are calculated to produce 1000 counts in the peak of the target image, which is the number of counts recommended for the non-critical ACQ/PEAK described above. The ACQ/PEAK sensitivity has considerable wavelength and aperture size dependence. A critical ACQ/PEAK into small apertures requires 10,000 counts total to achieve a centering error that corresponds to a signal loss of less than about 2%. For a critical peak up, the values in Table 2.1.2 relating to peak up must be multiplied by a factor of 10.

The times in Table 2.1.2 do not include the overhead involved in the initial setup of parameters or the analysis time, since that overhead should not be included on the Exposure Logsheet specifications.

Extrapolations of acquisition exposure times for sources fainter than V=19.5 should not be extrapolated from Table 2.1.2 because of the background noise.

2.2 Taking Spectra: ACCUM and RAPID Spectropolarimetry: STEP-PATT = POLSCAN

Examples of exposure logsheets are included for ACCUM mode (see lines 3.0 though 4.3) and RAPID mode (see lines 11.0 through 13.0).

In RAPID mode, when a wavelength range is specified, that range will be used whether or not there is room in memory for a larger region. Therefore, specifying a wavelength range is

Table 2.1.2
FOS Exposure Times (V = 15 unreddened)—Red Side

Spectral Type	$B-V$	Peak/up G190H	Peak/up G270H	Peak/up G400H	Peak/up G570H	Peak/up G780H	Peak/up G650L	Peak/up PRISM	Peak/up MIRROR	ACQ/BIN
07V	−0.32	0.1	0.1	0.2	0.4	2.9	0.3	0.1	0.1	0.39
B0V	−0.30	0.2	0.1	0.2	0.4	3.2	0.3	0.1	0.1	0.46
B1.5V	−0.25	0.2	0.1	0.2	0.4	3.0	0.4	0.1	0.1	0.53
B3V	−0.20	0.3	0.2	0.2	0.4	2.8	0.4	0.1	0.1	0.8
B6V	−0.15	0.4	0.2	0.2	0.4	2.9	0.4	0.1	0.1	1.0
B8V	−0.11	0.8	0.4	0.3	0.4	2.9	0.4	0.1	0.1	1.3
A1V	+0.01	2.3	0.9	0.4	0.4	2.7	0.4	0.2	0.2	2.0
A2V	+0.05	3.0	1.1	0.4	0.4	2.7	0.4	0.2	0.2	2.1
A6V	+0.17	5.3	1.4	0.4	0.5	2.6	0.4	0.2	0.2	2.4
A7V	+0.20	5.5	1.5	0.4	0.5	2.4	0.4	0.2	0.2	2.4
A9V	+0.28	10.0	1.8	0.5	0.5	2.3	0.5	0.2	0.2	2.7
F0V	+0.30	11.0	2.0	0.5	0.5	2.3	0.5	0.2	0.2	2.8
F5V	+0.44	19	2.1	0.5	0.5	2.1	0.5	0.3	0.2	3.0
F7V	+0.48	40	3.2	0.6	0.5	2.1	0.5	0.3	0.2	3.3
F8V	+0.52	46	3.8	0.6	0.5	2.0	0.5	0.3	0.3	3.4
G2V	+0.63	80	4.3	0.7	0.5	1.9	0.5	0.3	0.3	3.5
G6V	+0.70	—	4.6	0.7	0.5	1.9	0.6	0.3	0.3	3.7
K0V	+0.81	—	10.4	0.9	0.5	1.8	0.6	0.3	0.3	4.0
K0III	+1.00	—	24	1.2	0.5	1.7	0.6	0.4	0.3	4.5
K5V	+1.15	—	22	1.6	0.5	1.5	0.6	0.4	0.3	4.9
K4III	+1.39	—	80	2.3	0.5	1.5	0.7	0.5	0.4	5.4
M2I	+1.71	—	—	3.4	0.6	1.4	0.8	0.5	0.4	6.2
$\alpha = 1$		1.0	0.4	0.4	0.4	1.5	0.4	0.2	0.1	1.5
$\alpha = 2$		2.6	0.8	0.5	0.5	1.2	0.5	0.2	0.2	2.2
$\alpha = -2$	−0.46	0.1	0.1	0.2	0.4	2.8	0.3	0.1	0.1	0.23
$t = 50{,}000°$		0.1	0.1	0.2	0.4	2.7	0.3	0.1	0.1	0.35

FOS Exposure Times (V = 15 unreddened)—Blue Side

Spectral Type	Peak/up G130H	Peak/up G190H	Peak/up G270H	Peak/up G400H	Peak/up G570H	Peak/up G650L	Peak/up PRISM	Peak/up MIRROR	ACQ/BIN
07V	0.8	0.2	0.1	0.3	5.4	1.4	0.1	0.1	0.60
B0V	0.9	0.3	0.2	0.3	5.7	1.5	0.1	0.1	0.71
B1.5V	1.2	0.4	0.2	0.3	5.9	1.6	0.1	0.1	0.84
B3V	2.7	0.7	0.3	0.4	6.0	1.7	0.2	0.1	1.5
B6V	3.9	0.8	0.4	0.5	6.2	1.9	0.2	0.2	1.8
B8V	8.6	1.8	0.5	0.5	6.2	1.9	0.2	0.2	2.7
A1V	67.	4.9	1.3	0.7	6.7	2.3	0.3	0.3	5.0
A2V	—	6.4	1.6	0.7	6.4	2.3	0.4	0.4	5.6
A6V	—	11.	2.0	0.8	7.2	2.6	0.4	0.4	6.6
A7V	—	12.	2.1	0.9	7.2	2.7	0.5	0.5	7.0
A9V	—	21.	2.4	1.0	7.6	3.0	0.5	0.5	7.9
F0V	—	23.	2.7	1.0	7.8	3.2	0.5	0.6	8.4
F5V	—	37.	2.8	1.1	8.3	3.6	0.6	0.6	9.4
F7V	—	—	4.2	1.3	8.7	3.9	0.7	0.8	11.
F8V	—	—	5.1	1.4	8.7	4.1	0.8	0.8	12.
G2V	—	—	5.6	1.4	8.8	4.2	0.8	0.9	13.
G6V	—	—	5.8	1.6	9.3	4.8	0.9	0.9	14.
K0V	—	—	13.	1.9	9.6	5.2	1.2	1.2	18.
K0III	—	—	31.	2.9	10.	6.4	1.7	1.8	27.
K5V	—	—	28.	4.1	11.	8.2	2.2	2.4	36.
K4III	—	—	—	6.1	13.	11.	3.3	3.6	54.
M2I	—	—	—	9.2	16.	14.	4.5	5.1	77.
$\alpha = 1$	12.	2.0	0.6	0.7	7.9	2.9	0.3	0.2	3.3
$\alpha = 2$	41.	5.3	1.1	1.0	9.0	3.8	0.4	0.4	5.9
$\alpha = -2$	0.2	0.1	0.1	0.2	5.3	1.3	0.1	0.1	0.30
$T = 50{,}000°$	0.5	0.2	0.1	0.3	5.7	1.5	0.1	0.1	0.53

Notes to Table 2.1.2

Note: Exposure time must be multiplied by $10^{0.4(V-15)}$.

[1] Optimal exposure times for ACQ/BINARY and ACQ/FIRMWARE are calculated to detect 300 peak counts in the peak pixel of the target.

[2] ACQ/PEAK into the $0.2'' \times 1.2''$ (0.25X2.0) slit requires 10000 total counts.

[3] Exposure times for ACQ/PEAK into all apertures excluding the slit are calculated to detect 1000 total counts for non-critical acquisitions. For critical centering into small apertures, multiply the exposure times by a factor of 10. **Note that the exposure time for ACQ/PEAK must be multiplied by the inverse throughput of the aperture used (T_λ, see Figure 1.2.2).** Although the exact factor depends on the input spectrum, the approximate multiplicative factors are 1.1 for the $0.9''$ apertures (1.0), 1.2 for the $0.4''$ apertures (0.5), and 1.25 for the $0.3''$ aperture (0.3).

Table 2.1.3

Minimum Exposure Times to be Entered in Exposure Logsheets

ACQ/BINARY	0.66 sec
ACQ/FIRMWARE	0.96 sec
ACQ/PEAK	0.003 sec
ACQ	3.84 sec

??!!

not a good idea unless absolutely necessary, because it restricts the wavelength region that is read out. The full wavelength region is often useful. For example, the background can be determined directly from the diode array for gratings G130H, G160L, G190H, G650L, G780H, and PRISM. The diodes below the lowest wavelength, given in Table 1.1.1, can be used to average the actual background rate. The zero order can be monitored for G160L if all diodes are read out. If the observer needs *only* a specific wavelength range to be read out, then that range should be specified in with the keyword WAVELENGTH (column 8) of the Phase II exposure logsheet. Otherwise, the largest possible wavelength range will be automatically observed that is compatible with the READ-TIME requested.

The use of STEP-PATT = POLSCAN is demonstrated in the exposure logsheet lines 14.0 through 19.0. As mentioned in Section 1.5, only the G270H grating may be available for polarimetric observations post COSTAR.

3. INSTRUMENT PERFORMANCE AND CALIBRATIONS

ref to Our Book

3.1 Wavelength Calibrations

All FOS wavelengths are vacuum wavelengths, both below 2000Å and above.

Observations of the dwarf emission line star AU Mic, that have been corrected for geomagnetically induced image drift, are used to produce a measurement of the offsets in the wavelength scale between the internal calibration lamp and a known external point source (Kriss, Blair, & Davidsen 1992). On the red side, the mean offset between internal and external source is $+0.176 \pm 0.105$ diodes. On the blue side, the mean offset is -0.102 ± 0.100 diodes. These offsets are not included in the pipeline reduction wavelength calibration. With the observed dispersion reported by Kriss, Blair, & Davidsen, velocity measurements based on single lines in FOS spectra have a limiting accuracy of roughly 20 km s^{-1} if wavelength calibrations are obtained at the same time (*i.e.* NO GAP), and if the target is well centered in the science aperture. If simultaneous wavelength calibrations are not obtained, the non-repeatability in the positioning of the filter–grating wheel will dominate the errors in the zero point of the wavelength scale (Hartig, 1989).

3.2 Absolute Photometry

The absolute photometric calibration has been performed by observing the standard stars G191B2B (WD0501+527), BD+28D4211, BD+75D325, HZ–44, and BD+33D2642 several times in the large ($3.7'' \times 1.2''$, 4.3) aperture. The blue side calibrations of the G130H, G190H, G270H, G400H, G160L gratings, and the prism, all show an overall degradation of sensitivity of up to 10% in 1991, with a slower rate of degradation in 1992. The red side calibrations of the G190H, G270H, G400H, G570H, G780H, G160L, G650L gratings, and the prism, show sensitivity stable to within 5%, except in the region between 1800Å and 2050Å, where a trough is developing at the rate of 10–20% in 1991, with a slower rate of degradation in 1992 (Neill, Bohlin, & Hartig 1992).

Update

3.3 Flat Fields

get new SMOV superflats from Tony

Observations of two white dwarfs (G191B2B and KPD 0005+5106) were conducted to produce spectral flat fields for the principal FOS grating and detector combinations. Results of these tests are reported by Anderson (1992). The blue side flat fields display a typical standard deviation of the order of 1% about the mean value of unity (Figure 3.3.1). However, the red side is more problematical, exhibiting strong granularity in the G160L and the G190H gratings (Figures 3.3.2 and 3.3.3), and to a lesser extent, in the G270H grating. The granularity has increased between the first flat fields taken in October, 1990, and later flat fields taken in early 1992. The flat field obtained using the large aperture (taken in Cycle 2 in the $4.3'' \times 1.4''$ aperture) differs from the flat fields obtained using the other, smaller apertures. The red side flat field was monitored in the $4.3''$ for the three problematic gratings on a quarterly basis as part of the Cycle 2 calibration program to track any further changes in the red side flat fields. Because of the difference between the flat fields obtained using the large aperture versus the smaller apertures, flat fields were taken using both the large aperture and in the slit ($0.25'' \times 1.4''$).

Red side data taken after January 1992 can be flat fielded with the data most appropriate to the observation. The STSDAS task getreffile will refer the user to the appropriate flat field. Because getreffile refers to the Calibration Data Base System (CDBS) for temporal

If flat fields are to apply then acq must center the target as well as if was centered in all. Program

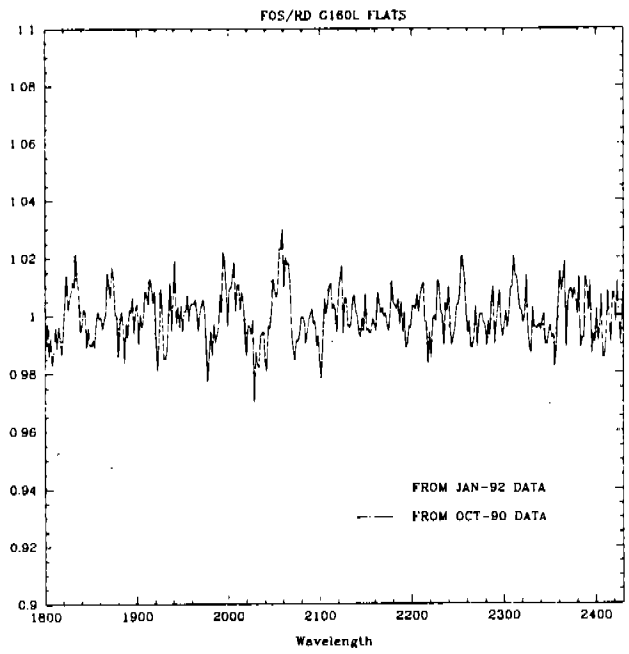

Figure 3.3.1: Redside G160L Flat Fields of target G191-B2B from October 1990 and January 26, 1992 data.

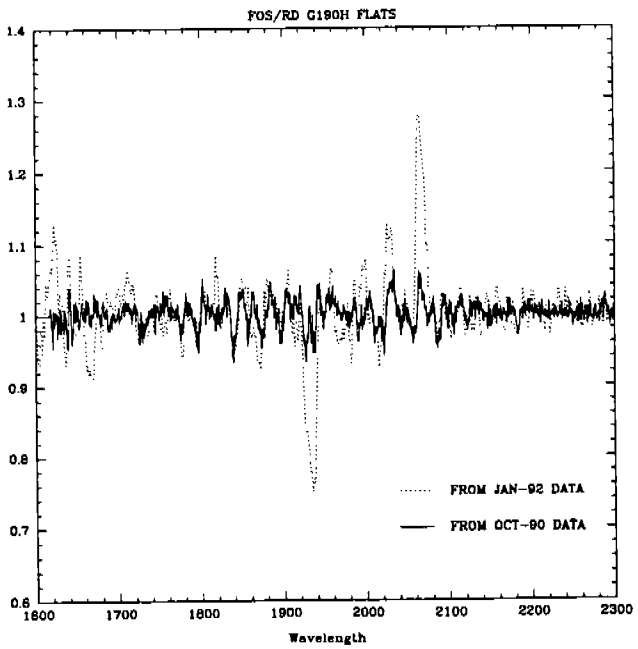

Figure 3.3.2: Redside G190H Flat Fields of target G191-B2B from October 1990 and January 26, 1992 data.

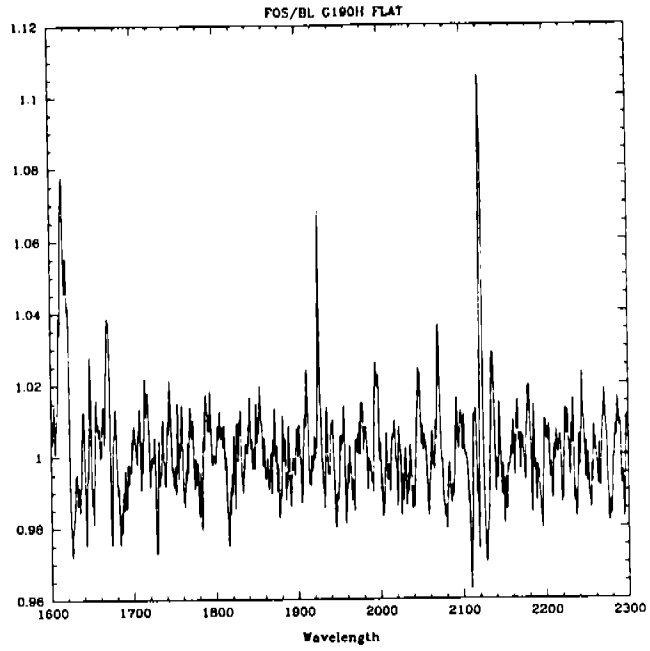

Figure 3.3.3: Blueside G190H Flat Field of target G191-B2B from September 1991.

information, the task is available only at ST ScI. For help with this task, observers can send requests to analysis@stsci.edu and ask that getreffile be run for the appropriate data set. Red side data taken between October 1990 and January 1992 will be difficult to flat field because of the lack of time–dependent flat fields available between 1990 and 1992.

3.4 Sky Lines

The lines of geocoronal Ly $\alpha\lambda$1216 and OI λ1304 appear regularly in FOS spectra, with a width determined by the size of the aperture (see Table 1.1.3). Occasionally, when observing on the daylight side of the orbit, the additional sky line of OII λ2470 can also be seen.

4. SIMULATING FOS

A simulator developed by K. Horne is available in the ST ScI Data Analysis System (STSDAS) in the package **synphot** (see ST ScI Newsletters Vol. 7, No. 2 and 3 for brief descriptions by K. Horne, and Synphot Users Guide, by D. Bazell, Nov. 1990, ST ScI.) XCAL, a version of the simulator which is compatible with VAX/VMS machines, can be copied from the ST ScI Electronic Information Service (STEIS) via an anonymous ftp account (for instructions on logging into STEIS, see Reppert, December 1990, ST ScI Newsletter Vol. 7, No. 3, page 16).

Synphot can be used to "observe" an interactively determined input spectrum with any FOS configuration to produce a spectrum of detector counts s^{-1} $diode^{-1}$. This can be done with the task **plspec**, by setting the observing mode, the input spectrum, the form of the output, and the wavelength dispersion of the output spectrum.

For example, to reproduce the counts s^{-1} $diode^{-1}$ plot for the blue side of grating G190H shown in Figure 1.2.3, the parameters for **plspec** would be set as given in Table 4.1, with the observing mode set with the parameter "obsmode = fos, blue, g190h, 4.3", the input spectrum set with the parameter "spectrum = flam 1.e-14," the units for the plot to be produced set by the parameter "form = counts", and the wavelength resolution of the resulting plot set with the parameter "wavetab = g190hb.dat".

The observing mode is simply the instrument (fos), followed by the side (red or blue), followed by the grating (of the gratings available in Table 1.1.1), followed by the aperture. The **form** of the plot can be **fnu** (F_ν = erg s^{-1} cm^{-2} Hz^{-1}), **flam** (F_λ = erg s^{-1} cm^{-2} $Å^{-1}$), **photnu** (detected counts s^{-1} cm^{-2} Hz^{-1}), **photlam** (detected counts s^{-1} cm^{-2} $Å^{-1}$), **counts** (detected counts s^{-1} cm^{-2} $pixel^{-1}$), or **abmag** (Magnitude = $-2.5\log(\text{fnu}) - 48.60$).

For calculating signal-to-noise ratio, **counts** is the best option for the parameter **form**, with a synphot "pixel" defined as a resolution element. When using **counts**, the pixel size is determined by the **wavetab** parameter. A series of tables are available which correspond to the wavelength dispersion of the diodes of the FOS gratings, where a diode is a resolution element. These tables are invoked with "wavetab=g190hb.tab", for example for the G190H grating on the blue side.

Synphot and XCAL also contain the stars in the Bruzual, Person, Gunn, & Stryker Atlas (not yet published) which covers a full range of spectral types (Bazell 1990).

A power law spectrum can also be input into **plspec**. For example, as a test, a power law of form $F_\nu \propto \nu^{-\alpha}$, with $\alpha = 2$, normalized to the value $F_\lambda = 1.0 \times 10^{-14}$ erg s^{-1} cm^{-2} $Å^{-1}$ can be used. This gives the same result as the case given in Table 4.1, with a constant value for F_λ, and thus demonstrates how to input a power law normalized to a flux in the ultraviolet. The command is "spectrum = pl 1900 2 rn "box 1900 1" flam 1.e-14." In this example, the power law is designated by **pl**, at 1900Å, with a slope of **-2**. This power law is renormalized "rn" to the bandpass 1Å wide at 1900Å which is defined in double quotes by **"box 1900 1"**. The renormalization value is given by "flam 1.e-14". The renormalization could have been given in any of the units available for the units of the plot.

Both **synphot** and XCAL use the updates to instrument sensitivities as they are produced.

Table 4.1
Example parameters in SYNPHOT to reproduce a spectrum with
Flux = 1.0 x10^{-14}, as in Figure 1.2.3

Parameter	Setting	Definition
obsmode	**fos,blue,g190h,4.3**	Observation mode or @filelist
spectrum	**flam 1.e-14**	Synthetic spectrum or @filelist
spfile	none	Spectrophotometry data
pfile	none	Photometry data
form	**counts**	Form for output graph
ebmv1	0.	First E(B-V) value
ebmv2	0.	Last E(B-V) value
nebmv	1.	Number of E(B-V) values
device	stdgraph	Output device
left	**1400.**	x value for left side of graph
right	**2400.**	x value for right side
bottom	**0.**	y value for bottom
top	**4.**	y value for top
errtype	n	n[one] p[oints] c[ontinuous] v[ertical] h[oriz]
wavetab	**g190hb.dat**	Wavelength table name
refdata		Reference data
mode	h	

Acknowledgements

I would like to thank Ralph Bohlin, Ian Evans, and Tony Keyes for their careful reading of the Handbook. I would also like to thank Tony Keyes for updating the FOS simulator, for producing both bright limits and target acquisition times, and for making many useful suggestions. I would like to thank Cindy Taylor for producing most of the tables and the plots, and Giselle Sleiman for producing the post-COSTAR PSF's and throughputs. I would like to thank Bram Boroson, Ross Cohen, Mingsheng Han, Buell Jannuzi, Vesa Junkkarinen, Ray Lucas, and Ruth Peterson for reading and commenting on the text. Finally, I would like to thank George Hartig for his advice and comments.

Rogier Windhorst Jan Christensen, Howard Richards,
Anne Connolly Pete Rapport

5. REFERENCES

Allen, R.G., & Angel, J.R.P. 1982, *FOS Spectropolarimeter Performance, FOS Instrument Handbook*, Version 1, ST ScI, page C-1.

Allen, R.G., & Smith, P.S. 1992, *FOS Polarimetry Calibrations*, Instrument Science Report CAL/FOS-078.

Anderson, S.F. 1992, *FOS Spectral Flat Field Calibration*, Instrument Science Report CAL/FOS-075.

Bazell, D. 1990, *Synphot Users Guide*, ST ScI.

Burrows, C., & Hasan, H. 1991, *Telescope Image Modelling User Manual*, ST ScI.

Caldwell, J., & Cunningham, C.C. 1992, *Grating Scatter in the FOS and the GHRS*, Science Verification 1343 Interim Report.

Ford, H.C. 1985, *FOS Instrument Handbook*, ST ScI.

Harms, R.J. 1982, *The Space Telescope Observatory*, ed. D.N.B. Hall, (Special Session of Commission 44, IAU General Assembly, Patras, Greece, August, 1982; NASA CP-2244).

Harms, R.J., Angel, R., Bartko, F., Beaver, E., Bloomquist, W., Bohlin,R., Burbidge, E.M., Davidsen, A.,F., Flemming, J.C., Ford, H., & Margon, B. 1979, *SPIE*, **183**, 74.

Hartig, G.F. 1989, *Faint Object Spectrograph Instrument Handbook Supplement No. 1*, ST ScI.

Hartig, G.F. 1989, *FOS Filter-Grating Wheel Repeatability: Dependence on Motor Selection*, Instrument Science Report CAL/FOS-060.

Kriss, G.A., Blair, W.P., & Davidsen, A.F. 1991, *In-Flight FOS Wavelength Calibration – Template Spectra*, Instrument Science Report CAL/FOS-067.

Kriss, G.A., Blair, W.P., & Davidsen, A.F. 1992, *Internal/External Offsets in the FOS Wavelength Calibration*, Instrument Science Report CAL/FOS-070.

Lindler, D., & Bohlin, R. 1986, *FOS Linearity Corrections*, Instrument Science Report CAL/FOS-025.

Morris, S.L., Weymann, R.J., Savage, B.D., & Gilliland, R.L. 1991 *Ap. J. (Letters)*, **377**, L21.

Mount, G., & Rottman, G. 1981, *The Solar spectral irradiance 1200–3184Å near solar maximum: July 15, 1980*, J. Geophys. Res. **86**, 9193.

Neill, J.D., Bohlin, R.C., & Hartig, G. 1992, *Photometric Calibration of the Faint Object Spectrograph*, Instrument Science Report CAL/FOS-077

Rosenblatt, E.I., Baity, W.A., Beaver, E.A., Cohen, R.D., Junkkarinen, V.T., Linsky, J.B., and Lyons, R.W. 1992, *An Analysis of FOS Background Dark Noise*, Instrument Science Report CAL/FOS-071.

Wegener, R., Caldwell, J., Owne, T., Kim, S.J., Encrenaz, T., & Comber, M. 1985 *The Jovian Stratosphere in the Ultraviolet, Icarus*, **63**, 222.

APPENDIX A.

Taking Data with FOS

To ensure that the user is always confused, two sets of nomenclature are used to describe the taking of FOS data—those used in the exposure logsheets to command observations, and those used in the FOS data headers. Table A.1 gives the translation between the two, together with defaults and definitions.

FOS observations are performed in a nested manner, with the innermost nest being the livetime of the instrument plus the deadtime (LT + DT). Table A.1 lists the parameters in the order in which FOS observations are nested. Standard spectra are taken by sub–stepping the diode array along the dispersion in the X direction, and then by performing the sub–stepping five times over adjacent diodes to minimize the impact of dead diodes. The sequence is then

$$(\mathrm{LD} + \mathrm{DT}) \times 4 \times 5.$$

The minimum livetime is 0.003 seconds. The minimum livetime plus deadtime is 0.030 seconds. Using the minimum livetime results in very inefficient observations, since data are being taken only $0.003/0.03 = 0.1$ of the time.

The user has access only to those parameters that can be set in the exposure logsheet. For example, the user cannot set the livetime, but the user can set the product of livetime and INTS (**STEP-TIME** = LT× INTS). Likewise, the user cannot explicitly set the deadtime, but in **PERIOD** mode, the user can set the ratio of livetime to deadtime (**DATA-RATIO** = LT/DT).

For the most common mode, **ACCUM**, an FOS integration is constructed in the order (LT+DT), INTS, NXSTEPS, OVERSCAN, YSTEPS, NPATT, and finally NREAD. The total elapsed time of an integration is then given by

$$\Delta t = (\mathrm{LT} + \mathrm{DT}) \times \mathrm{INTS} \times \mathrm{NXSTEPS} \times \mathrm{OVERSCAN} \times \mathrm{YSTEPS} \times \mathrm{NPATT} \times \mathrm{NREAD}.$$

where NXSTEPS = **SUB-STEP**, and YSTEPS = **Y-SIZE**. This equation also gives the elapsed time for the observation, which for standard **ACCUM** mode is equal to

$$\Delta t = (\mathrm{LT} + \mathrm{DT}) \times \mathrm{INTS} \times 4 \times 5 \times 1 \times \mathrm{NPATT} \times \mathrm{NREAD}.$$

The number of patterns, NPATT, is set after the setting of sub–step (NXSTEPS), OVSERSCAN, and YSTEP, to achieve the exposure time requested. When NPATT has reached the maximum that it can be set to (256), then INTS is incremented. Obviously, this must be done in an optimal way to ensure that the efficiency ($\propto$ LT/DT) remains high. The maximum value for INTS is also 256.

For a **RAPID** observation, an FOS integration is built up in a slightly different order; (LT+DT), INTS, NXSTEP, OVERSCAN, YSTEPS, NPATT, and finally NMCLEARS. The total elapsed time of the observation is

$$\Delta t = (\mathrm{LT} + \mathrm{DT}) \times \mathrm{INTS} \times \mathrm{NXSTEP} \times \mathrm{OVERSCAN} \times \mathrm{YSTEPS} \times \mathrm{NPATT} \times \mathrm{NMCLEARS}.$$

which is usually equal to

$$\Delta t = (\mathrm{LT} + \mathrm{DT}) \times \mathrm{INTS} \times 4 \times 5 \times 1 \times \mathrm{NPATT} \times \mathrm{NMCLEARS}.$$

However, the sub–stepping, the overscan values, and the wavelength range can be lowered in RAPID to accommodate shorter time between the taking of spectra.

For a PERIOD observation, an FOS integration is built up of

$$\Delta t = (\mathrm{LT} + \mathrm{DT}) \times \mathrm{INTS} \times \mathrm{NXSTEP} \times \mathrm{OVERSCAN} \times \mathrm{YSTEPS} \times \mathrm{SLICES} \times \mathrm{NPATT}$$

where SLICES = BINS. As with RAPID, x step and overscan values can be lowered to result in a greater number of SLICES (BINS).

These equations give the elapsed time of an observation and so they can be used to calculate the actual start time of any observation, by subtracting them from the first packet time (FPKTTIME) which is given in the group parameter at the beginning of every group of "multi–group" data.

$$\text{Start Time} = \mathrm{FPKTTIME} - \Delta t$$

The start time of the entire observation is also given in the data header as EXPSTART. Note that all times in the header, including the first packet time, and the start time, are given in units of Modified Julian Date, which is the Julian date minus 2400000.5. The Modified Julian Date for 1993 is given by:

$$\mathrm{MJD} = 48987.0 + \text{day of year} + \text{fraction of day from } 0^h UT.$$

Table A.1

FOS Observing Parameters
Listed in Order of Execution

Exposure Logsheet	FOS Header	Default	Definition
—	LIVETIME	0.500 sec	(LT) Time FOS is integrating.
—	DEADTIME	0.010 sec	(DT) Overhead time.
—	INTS	—	Number of times to execute (LT+DT)
SUB-STEP	NXSTEP	4	Number of steps of size diode/NXSTEP in direction of dispersion.
COMB	OVERSCAN*	YES	Whether or not to execute x stepping to remove the effects of dead diodes. For COMB= YES, MUL=5. For COMB= NO, MUL=1.
Y-SIZE	YSTEPS	1	Number of steps perpendicular to dispersion.
BINS	SLICE	5	For PERIOD only, equal to 1 otherwise. Number of bins to divide one period into.
—	NPATT	—	Number of times to execute the pattern so as to achieve the exposure time.
—	NREAD	—	For ACCUM only, equal to 1 otherwise. For readouts short enough to correct for GIMP
—	NMCLEARS	—	For RAPID only, equal to 1 otherwise. Number of times to clear data so as to read new data.

* The FOS header value for OVERSCAN is equal to the value for MUL.

Additional FOS Observing Parameters

Exp.Log.	FOS	Default	Definition
STEP-TIME	LT×INTS	0.5	Available in RAPID and PERIOD.
DATA-RATIO	LT/DT	Maximum	Available in PERIOD only.

APPENDIX B.

Dead Diode Tables

Occasionally one of the 512 diodes on the red or the blue side becomes very noisy, or ceases to collect data. Since launch, the FOS has lost 3 diodes on the blue side and 2 diodes on the red side. In addition, several diodes on each side have become noisy and have been disabled. When a diode goes bad in orbit, there is a delay before that diode behavior is discovered, and another delay time before that diode is disabled so that its effect is removed from the data. Table B.1 lists the current (as of January 18, 1993) list of disabled diodes. Table B.2 lists the history of the diodes that have been disabled, when they were discovered to be bad, and when they were removed from action. Note that the channels are numbered in this table from 0 to 511, while they are numbered in the STSDAS tasks from 1 to 512.

Table B.1
FOS DEAD AND NOISY CHANNEL SUMMARY[1]

BLUE DETECTOR

DISABLED Dead Channels	DISABLED Noisy Channels	DISABLED Cross-Wired Channels	ENABLED But Possibly Noisy
49	31	47	8
101	73	55	426
223	201		
284	218		
409	225		
441	235		
471	241		
	268		
	398		
	415		
	427		
	451		
	465		
	472		
	497		

RED DETECTOR

DISABLED Dead Channels	DISABLED Noisy Channels	ENABLED But Possibly Noisy
2	110	153
6	189	174
29	285	261
197	380	410
212	405	412
486	409	

1. Diode range is 0-511.

Table B.2
FOS DEAD AND NOISY CHANNELS HISTORY[1]

BLUE DETECTOR

DISABLED Dead Channels	DATE Died	DATE Disabled
49	2/17/88	2/17/88
101	8/28/91	12/14/91
223	4/6/88	4/6/88
284	2/17/88	2/17/88
409	2/17/88	2/17/88
441	6/20/91	8/3/91
471	6/1/91	8/3/91

DISABLED Noisy Channels	DATE Noticed	DATE Disabled
31	3/11/88	11/1/90
73	Prelaunch	Prelaunch
201	Prelaunch	Prelaunch
218	Prelaunch	Prelaunch
225	?	5/18/90,(enabled 6/11/90),11/1/90
235	10/1/90	11/1/90
241	10/3/90	11/1/90
268	Prelaunch	Prelaunch
398	12/90	2/20/91
415	10/92	Prelaunch,(enabled 2/20/91),2/8/93
427	3/5/92	Prelaunch,(enabled 2/20/91),4/13/92
451	Prelaunch	Prelaunch
465	Prelaunch	Prelaunch
472	Prelaunch	Prelaunch
497	3/11/88	11/1/90
219	Prelaunch	Prelaunch,ENABLED 2/20/91

RED DETECTOR

DISABLED Dead Channels	DATE Died	DATE Disabled
2	Prelaunch	Prelaunch
6	Prelaunch	Prelaunch
29	10/27/91	1/7/92
197	12/90	2/20/91
212	Prelaunch	Prelaunch
486	Prelaunch	Prelaunch

DISABLED Noisy Channels	DATE Noticed	DATE Disabled
110	7/16/90	9/14/90
189	9/91	12/14/91
285	Prelaunch	Prelaunch (formerly DEAD)
380	7/91	8/3/92
405	Prelaunch	Prelaunch
409	Prelaunch	Prelaunch
235	Prelaunch	Prelaunch,ENABLED 8/27/90
261	Prelaunch	Prelaunch,ENABLED 8/27/90
344	Prelaunch	Prelaunch,ENABLED 8/27/90
381	Prelaunch	Prelaunch,ENABLED 8/27/90

1. Diode range is 0-511.

APPENDIX C.

A Comparison of GHRS and FOS Sensitivities

R. Gilliland & G.F. Hartig

from ST ScI Newsletter, Nov. 1991, Vol. 8, no. 3, p. 13

To facilitate changes that may be necessary for Cycle 1 proposals that currently use the GHRS side 1 low-resolution grating, G140L, but will be changed to the FOS, the following table provides a direct comparison of GHRS and FOS photometric sensitivities for point sources well centered in the aperture.

The sensitivities in columns 2, 3, and 4 are expressed in counts^{-1} diode^{-1} per (erg s^{-1} cm^{-2} Å^{-1}).

For the GHRS with the G140L grating, column 2 gives the sensitivity with the 2.″0 square Large Science Aperture (LSA). For observations with the Small Science Aperture (SSA), the GHRS sensitivity should be multiplied by the ratio in the final column. With G140L the diode spacing is 0.572 Å, and the resolutions of the SSA and LSA are 1.1 and 2.0 diodes, respectively.

The FOS sensitivities are also on a per–diode basis, for the 1.″0—diameter circular aperture. The diode spacings are 1.0Å and 1.46Å for the G130H and G190H gratings, respectively, and the resolution of the 1.″0 aperture is 1.4 diodes.

A sample calculation: at 1200Å, one would infer from the above that GHRS G140L was a factor of 5 faster than FOS *on a per–diode basis.* On a per–Ångstrom basis, the ratio at 1200Å is 8.9. But the FOS does have greater wavelength coverage, and starts gaining ground rapidly with increasing wavelength in terms of relative sensitivity.

Throughputs for the various FOS apertures at 1500 Å, as determined from direct comparison on a point source, are as follows:

Aperture (arcsec)	Throughput (pre-COSTAR)
1.4×4.3	49%
1.0	27%
0.5	20%
0.3	13%
0.25×1.4	20%

The GHRS to FOS ratios derived from the table should typically be within 20% of truth, allowing for good exposure–time planning.

C Estimation of scattered light

Table C.1
GHRS and FOS Sensitivities Pre-COSTAR

Wavelength	GHRS G140L[a]	FOS/BL G130H	FOS/BL G190H	GHRS SSA/LSA[b]
1100	1.81×10^{11}[c]	0.00	-	0.19
1150	2.90×10^{12}	2.79×10^{11}	-	0.20
1200	7.75×10^{12}	1.53×10^{12}	-	0.21
1250	1.28×10^{13}	3.47×10^{12}	-	0.22
1300	1.45×10^{13}	4.57×10^{12}	-	0.22
1350	1.53×10^{13}	5.70×10^{12}	-	0.23
1400	1.45×10^{13}	6.50×10^{12}	-	0.23
1450	1.18×10^{13}	7.90×10^{12}	-	0.24
1500	9.24×10^{12}	9.41×10^{12}	-	0.24
1550	7.35×10^{12}	1.16×10^{13}	-	0.25
1600	5.27×10^{12}	1.37×10^{13}	1.83×10^{13}	0.25
1650	4.61×10^{12}	-	2.19×10^{13}	0.26
1700	3.79×10^{12}	-	2.50×10^{13}	0.26
1750	2.41×10^{12}	-	2.89×10^{13}	0.27
1800	1.25×10^{12}	-	3.45×10^{13}	0.27
1850	4.39×10^{12}	-	3.90×10^{13}	0.28
1900	1.29×10^{11}	-	4.50×10^{13}	0.28

a. This is for the LSA (2.0 arcsec square)
b. This is the expected SSA/LSA sensitivity.
c. All sensitivites are in: $\frac{\text{cts/s/diode}}{\text{ergs/s/cm}^2\text{/A}}$

APPENDIX D.

Grating Scatter

This appendix reports the results of tests analyzed by Caldwell & Cunningham (1992) on the red scattered light which contaminates blue side observations of FOS.

The FOS blue side detector is sensitive to visible wavelengths (see Figure 1.0.1) and is therefore susceptible to grating scatter. Grating scatter significantly affects FOS spectra of red objects below 2100Å. Grating scatter tests (Caldwell & Cunningham 1992) compare GHRS spectra in the G140L (central wavelength 1700Å), G270M (2300–3220Å), and G200M (1800–2185Å) gratings with FOS blue side observations of G190H (1570–2330), G270H (2230–3300Å), and G160L (1150–2520Å). Because GHRS is solar blind, the spectra produced by GHRS can show the degree to which red scattered light impacts blue spectra taken with the FOS. Although the test was done with the blue side, the red side of FOS, which has a higher blue sensitivity than the blue side and no attenuation of red sensitivity, has an appreciably greater scatter problem.

The G2V star 16 Cyg B was observed. Because 16 Cyg B is a solar analog, the solar spectrum can be used for an approximate independent check on the HST observations of 16 Cyg B. 16 Cyg B is determined to be a solar analog at wavelengths longer than 3000Å, so it may be intrinsically different than the sun in the ultraviolet. The spectra of 16 Cyg B from GHRS, and FOS, and the Solar spectrum from a rocket by Mount and Rottman (1981) is shown in the Figure D.1, reproduced from Caldwell, and Cunningham (1992). As can be seen in Figure D.1, the flux in the FOS spectrum increases strongly toward wavelengths below 2100Å relative to the true flux. This is because the blue spectrum decreases rapidly with shorter wavelengths, so the relative contribution from scattered light increases towards shorter wavelength.

App D.

Fos Wavelength Comparison Spectra

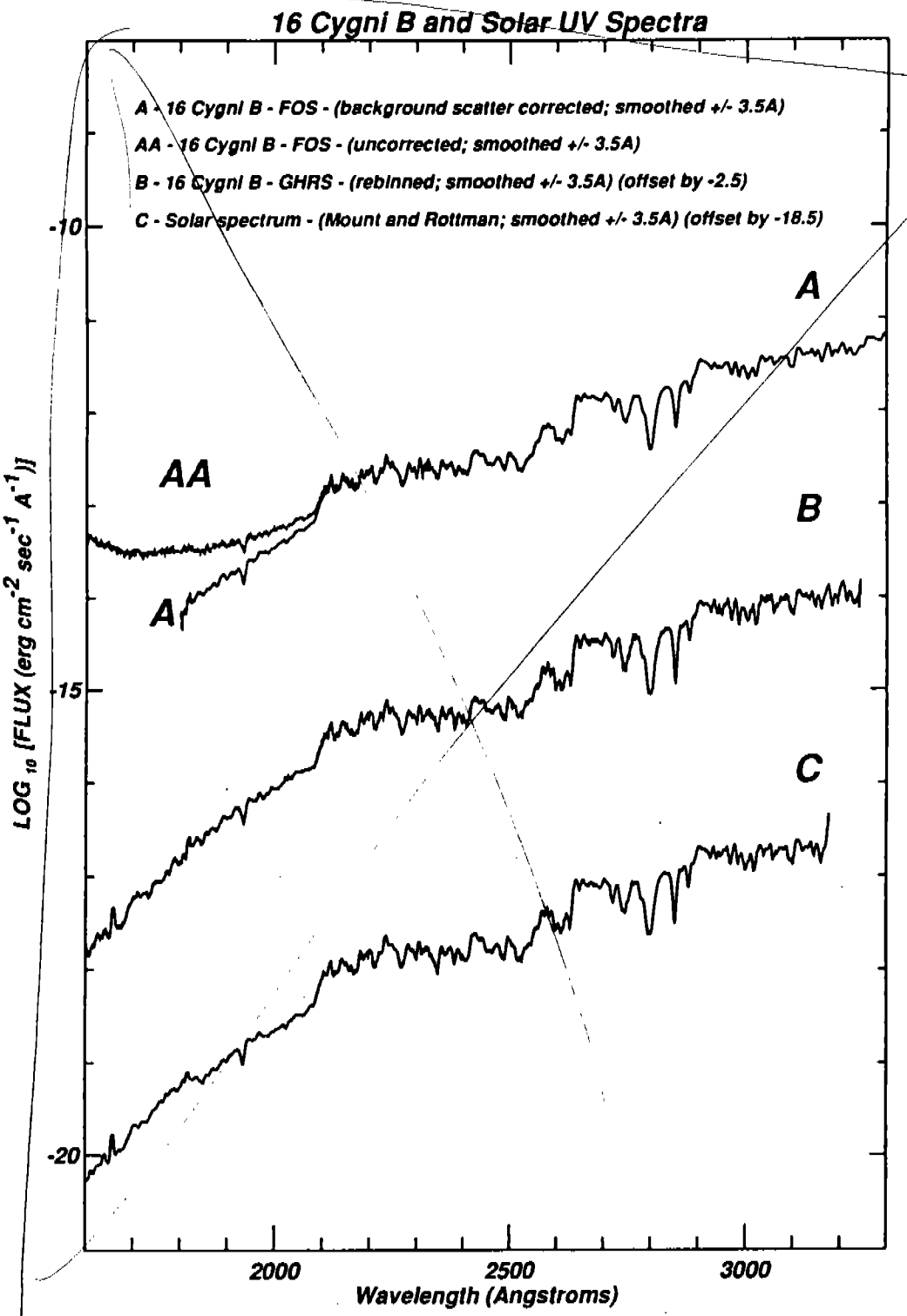

Figure D.1: Comparison of FOS and GHRS 16 Cyg B HST spectra with a solar rocket UV spectrum by Mount and Rottman (1981), as modified by Wagener *et al.* (1985). The FOS uncorrected spectrum (curve AA) is a composite of the G190H and G270H FOS observations. Curve A is a replot of these data after a correction for grating scatter has been applied. A composite spectrum of all the GHRS spectra is plotted as curve B. The modified Mount and Rottman (1981) solar data is plotted as curve C.

APPENDIX E

Faint Object Spectrograph Instrument Science Reports

January 27, 1993

060 FOS Filter-Grating Wheel Repeatability: Dependence on Motor Selection , G. Hartig - 5/89

067 In-Flight FOS Wavelength Calibration - Template Spectra G.A. Kriss, W.P. Blair, and A.F. Davidsen - 2/91

068 FOS Red Detector Plate Scale and Orientation, B. Bhattacharya and G. Hartig - 11/91

069 FOS Red Detector Flat-field and Sensitivity Degradation, G. Hartig - 11/91

070 Internal/External Offsets in the FOS Wavelength Calibration G.A. Kriss, W.P. Blair, and A.F. Davidsen - February 1992

071 An Analysis of FOS Background Dark Noise - E.I. Rosenblatt, W.A. Baity, E.A. Beaver, R.D. Cohen, V.T. Junkkarinen, J.B. Linsky, and R. Lyons - 4/92

072* Aperture Calibrations During Science Verification of the FOS L. Dressel and R. Harms - May 1992 (reworked)

073 Scattered Light Characteristics of the HST FOS F. Bartko, G.S. Burks, G. A. Kriss, A.F. Davidsen, R.D. Cohen, V.T. Junkkarinen and R. Lyons - April 1992

074 On - Orbit Discriminator Settings for FOS R.D. Cohen - February 1992

075 FOS Spectral Flat Field Calibration (Science Verification Phase Data), S.F. Anderson - February 1992

076 Analysis of FOS On-Orbit Detector Background with Burst Noise Rejection, E.A. Beaver and R. W. Lyons - April 1992

077 Photometric Calibration of the FOS J. D. Neill, R. C. Bohlin, and G. Hartig - June 1992

078 FOS Polarimetry Calibration [update of CAL/FOS 055] R.G. Allen and P.S. Smith - March 1992

079 FOS Operation in the South Atlantic Anomaly W. A. Baity, E. A. Beaver, J.B. Linsky and R. W. Lyons - April 1992

080 FOS On-Orbit Background Measurements R. W. Lyons, J. B. Linsky, E.A. Beaver, W. A. Baity, and E. I. Rosenblatt - April 1992

081 FOS Onboard Target Acquisition Tests S. Caganoff, Z. Tsvetanov, and L. Armus - April 1992

082 Lab Test Results of the FOS Detector Performance in a Variable External Magnetic Field E. A. Beaver and P. Foster - June 1992

084 Photometric Calibration of the Faint Object Spectrograph and Other JST Scientific Instruments - R.C. Bohlin and J.D. Neill 7/92

085 FOS Aperture Throughput Variations with OTA Focus - D. Lindler and R. Bohlin, 8/92

086 Analysis of Photometric Standards following July 1992 FOS Overlight Stafing Event, C. J. Taylor and C. D. Keyes, 12/92

* Draft version - not yet released.

APPENDIX F

Exposure Logsheets

The RPS version of the Exposure Logsheets given in Appendix F can be copied from anonymous ftp (stsci.edu, or 130.167.1.2). The Logsheets are in the subdirectory proposer/documents/props_library. They are called fos_handbook4_example.

FIXED TARGET EXAMPLE

1 TAR NUM	2 TARGET NAME	3 TARGET DESCRIPTION	4 TARGET POSITION	5 COORD EQNX	6 PM PR	7 RADIAL VEL.	8 ACQUI PRBLM	9 SPEC PLATE RQ AV	FLX REF	10 FLUX DATA
1	3C298 QUASAR	E,314	RA-OFF= 8.785' +/- 0.3", DEC-OFF= 20.9' +/- 0.3", FROM 2						1	V= 16.79, E(B-V)= 0.2
2	3C298-OFFSET COMMENTS: A5 STAR USED FOR OFFSET.	A,126	RA= 14H 16M 30S +/- 1", DEC= +6D 42' 0" +/- 1"	1950					1	V=15
3	M81	E,301,919	RA= 9H 51M 30S +/- 10", DEC= +69D 18.3' +/- 10"	1950					1	V=18,E(B-V)=0.2
4	M81-OFFSET COMMENTS: TO BE FOUND - OFFSET STAR.	A	RA-OFF= 0.05S +/- 1', DEC-OFF= 0' +/- 1, FROM 3, TBD-EARLY							
5	BRIGHT_STAR	A,111	RA= 2H 16M 28S +/- 1", DEC= +43D 51' 56" +/- 2"	1950					1	V=14,TYPE-B3V,E(B-V)=0.5
6	AE-AQR	A,151,154,161	RA= 20H 40M 9.02S +/- 0.5", DEC= -0D 52' 15.5" +/- 0.5", PLATE-ID=02C4	J2000	N				1	V= 10.8 +/- 1.1
7	0405-123	E,314	RA= 4H 5M 27.45S +/- 1", DEC= -12D 19' 31.8" +/- 1"	1950					1	V=14.82
8	MRK421	E,316	RA= 11H 1M 40.57S +/- 1", DEC= +38D 28' 43" +/- 1"	1950					1	V=13.5
9	WD0501+527 G191-B2B GS SS3734-0506 COMMENTS: THE GUIDE STAR CATALOG NAME IS GIVEN.	J,705,702	RA=05H 05M 30.6S +/- 0.01S, DEC=+52D 49' 54.0" +/- 0.2"	2000	Y				1 2 3	V = 11.78 +/- 0.02 B = 11.44 +/- 0.02 U = 10.24 +/- 0.02

Get rid of some * 4 stage pick up.

Add some:

See Tony's copy page 59

4 sl

Proper Motion/Parallax Form

Target number	Target name	Epoch of position		Proper motion in RA (arc-sec/yr)/cos(DEC)		Proper motion in DEC (arc-sec/yr)		Annual Parallax (arc-sec)	
		B/J	Year	value	uncertainty	value	uncertainty	value	uncertainty
8	WD0501+527 G191-B2B GSSS3734-0506	J	1983.10	0.0045	0.0030	-0.0880	0.0050	0.0000	0.0000

EXPOSURE LOGSHEET EXAMPLE

1 LN NM	2 SEQ NAME	3 TARGET NAME	4 INSTR CONFIG	5 OPER. MODE	6 APER OR FOV	7 SPECTRAL ELEMENT	8 CENTRAL WAVELN	9 OPTIONAL PARAMETERS	10 NUM EXP	11 TIME	12 S/N	13 FLX REF	14 PR	15 SPECIAL REQUIREMENTS
1.000		3C298-OFFSET	FOS/RD	ACQ/BINARY	4.3	MIRROR			1	2.41S		1	3	ONBOARD ACQ FOR 2 ; CYCLE 4 / 1-15;
2.000		3C298	FOS/RD	ACCUM	0.5	G780H	7800		1	600S	10	1	3	
	COMMENTS: SIGNAL_TO_NOISE IS PER DIODE.													
3.000		MRK421	FOS/RD	ACQ/BINARY	4.3	MIRROR		BRIGHT=57500, FAINT=1100,	1	0.66S		1	3	ONBOARD ACQ FOR 4 ; GROUP 3-4.3 NO GAP;
	COMMENTS: BLUE SIDE ACQ BIN- EXP=0.83 SEC. USE DEFAULT BRIGHT AND FAINT LIMITS.													
4.000		MRK421	FOS/RD	ACQ/PEAK	0.25X2.0	G190H		SCAN-STEP-X=.057, SEARCH-SIZE-X=7, SEARCH-SIZE-Y=1,	1	0.3S			1	ONBOARD ACQ FOR 4 .1-4.3;
4.100		MRK421	FOS/RD	ACCUM	0.25X2.0	G190H			1	300S			1	
4.200		MRK421	FOS/BL	ACQ/PEAK	0.25X2.0	G190H		SCAN-STEP-X=.057, SEARCH-SIZE-X=7, SEARCH-SIZE-Y=1,	1	0.6S			1	ONBOARD ACQ FOR 4 .3;
4.300		MRK421	FOS/BL	ACCUM	0.25X2.0	G130H			1	300S			1	
5.000		M81	WFC	IMAGE	ALL	F606W			1	60S		1	1	EARLY ACQ FOR 6-8 .1;
6.000		M81-OFFSET	FOS/BL	ACQ/BINARY	4.3	MIRROR			1	TBD		1	1	SEQ 6-8.1 NO GAP ONBOARD ACQ FOR 7 -8.1;
7.000		M81	FOS/BL	ACCUM	0.3	G190H	1900		1	3000S	10	1	1	
	COMMENTS: SIGNAL_TO_NOISE IS PER DIODE.													
8.000		M81	FOS/BL	ACQ	4.3	MIRROR			1	200S		1	1	
	COMMENTS: FOS ACQIMAGE OF FIELD OF VIEW.													

1 LN NM	2 SEQ NAME	3 TARGET NAME	4 INSTR CONFIG	5 OPER. MODE	6 APER OR FOV	7 SPECTRAL ELEMENT	8 CENTRAL WAVELN	9 OPTIONAL PARAMETERS	10 NUM EXP	11 TIME	12 S/N	13 FLX REF	14 PR	15 SPECIAL REQUIREMENTS
8.100		M81	FOS/BL	IMAGE	0.3	G400H		Y-SIZE=3, Y-SPACE=10.7, COMB=YES, SUB-STEP=4,	1	3600S	10		1	
	COMMENTS: SIGNAL_TO_NOISE IS PER PIXEL.													
10.300		BRIGHT_STAR	FOS/RD	ACQ/PEAK	4.3	G570H	5700	SCAN-STEP-Y=1.204, SEARCH-SIZE-X=1, SEARCH-SIZE-Y=3,	1	0.17S			1	ONBOARD ACQ FOR 1 0.4;
10.400		BRIGHT_STAR	FOS/RD	ACQ/PEAK	1.0	G570H	5700 .602	SCAN-STEP-X=.602, SCAN-STEP-Y=.300, SEARCH-SIZE-X=6, SEARCH-SIZE-Y=2,	1	0.18S			1	ONBOARD ACQ FOR 1 0.5;
10.500		BRIGHT_STAR	FOS/RD	ACQ/PEAK	0.5	G570H	5700	SCAN-STEP-X=0.30, SCAN-STEP-Y=0.30, SEARCH-SIZE-X=3, SEARCH-SIZE-Y=3,	1	0.19S			1	ONBOARD ACQ FOR 1 0.6;
10.600		BRIGHT_STAR	FOS/RD	ACCUM	1.0	G570H	5700		1	1M			1	
11.000		AE-AQR	FOS/BL	ACQ/PEAK	4.3	G190H		SCAN-STEP-Y=1.204, SEARCH-SIZE-X=1, SEARCH-SIZE-Y=3,	1	0.07S		1	1	ONBOARD ACQ FOR 1 1.1;
	COMMENTS: VARIABLE TARGET. FAINTEST V MAG USED WITH 13,000 BB IN SIMULATION. EXPECT MIN 1000 COUNTS/DWELL.													
11.100		AE-AQR	FOS/BL	ACQ/PEAK	1.0	G190H	.602	SCAN-STEP-X=.602, SCAN-STEP-Y=.300, SEARCH-SIZE-X=6, SEARCH-SIZE-Y=2,	1	0.08S		1	1	ONBOARD ACQ FOR 1 1.2;
11.200		AE-AQR	FOS/BL	ACQ/PEAK	0.3	G190H		SEARCH-SIZE=4, SCAN-STEP=0.25,	1	0.09S		1	1	ONBOARD ACQ FOR 1 1.3;

1 LN NM	2 SEQ NAME	3 TARGET NAME	4 INSTR CONFIG	5 OPER. MODE	6 APER OR FOV	7 SPECTRAL ELEMENT	8 CENTRAL WAVELN	9 OPTIONAL PARAMETERS	10 NUM EXP	11 TIME	12 S/N	13 FLX REF	14 PR	15 SPECIAL REQUIREMENTS
11.300		AE-AQR	FOS/BL	ACQ/PEAK	0.3	G190H		SEARCH-SIZE-X=5, SEARCH-SIZE-Y=5, SCAN-STEP-X=0.06, SCAN-STEP-Y=0.06,	1	0.90S		1	1	ONBOARD ACQ FOR 12;
	COMMENTS: CRITICAL ACQ/PEAK STAGE. EXP TO PRODUCE 10000 COUNTS/DWELL.													
12.000		AE-AQR	FOS/BL	RAPID	0.3	G190H		READ-TIME=4,	1	300M			1	
13.000		WD0501+527	FOS/RD	ACQ/PEAK	4.3	G270H		SCAN-STEP-Y=1.204, SEARCH-SIZE-X=1, SEARCH-SIZE-Y=3,	1	3.0S			1	ONBOARD ACQ FOR 13.1;
13.100		WD0501+527	FOS/RD	ACQ/PEAK	1.0	G270H	.602	SCAN-STEP-X=.602, SCAN-STEP-Y=~~301~~, SEARCH-SIZE-X=6, SEARCH-SIZE-Y=2,	1	3.0S			1	ONBOARD ACQ FOR 13.2;
13.200		WD0501+527	FOS/RD	ACQ/PEAK	0.5	G270H		SEARCH-SIZE-X=3, SEARCH-SIZE-Y=3, SCAN-STEP-X=0.30 SCAN-STEP-Y=0.30	1	3.0S		1	1	ONBOARD ACQ FOR 13.3;
13.300		WD0501+527	FOS/RD	ACQ/PEAK	0.3	G270H		SEARCH-SIZE-X=4, SEARCH-SIZE-Y=4, SCAN-STEP-X=0.125, SCAN-STEP-Y=0.125,	1	3.0S		1	1	ONBOARD ACQ FOR 13.4;
13.400		WD0501+527	FOS/RD	ACCUM	0.5	G270H			1	276S			1	
14.000		0405-123	FOS/BL	ACQ/BINARY	4.3	MIRROR			1	2.8S	17	13	1	ONBOARD ACQ FOR 15; SEQ 14-15 NO GAP;
15.000		0405-123	FOS/BL	ACCUM	4.3	G270H	2700	POLSCAN=4B	1	5H	90	13	1	

Get rid of some

Add some

```
EXAMPLE RPS :
-------------

FIXED_TARGETS:


 TARGNUM:                1
   NAME_1:               3C298
   NAME_2:               QUASAR
   DESCR_1:              E,314
   POS_1:                RA-OFF= 8.785' +/- 0.3",
   POS_2:                DEC-OFF= 20.9' +/- 0.3",
   POS_3:                FROM 2
   FLUXNUM_1:            1
   FLUXVAL_1:            V= 16.79, E(B-V)= 0.2


 TARGNUM:                2
   NAME_1:               3C298-OFFSET
   DESCR_1:              A,126
   POS_1:                RA= 14H 16M 30S +/- 1",
   POS_2:                DEC= +6D 42' 0" +/- 1"
   EQUINOX:              1950
   FLUXNUM_1:            1
   FLUXVAL_1:            V=15
   COMMENT_1:            A5 STAR USED FOR OFFSET.


TARGNUM:                 3
   NAME_1:               M81
   DESCR_1:              E,301,919
   POS_1:                RA= 9H 51M 30S +/- 10",
   POS_2:                DEC= +69D 18.3' +/- 10"
   EQUINOX:              1950
   FLUXNUM_1:            1
   FLUXVAL_1:            V=18,E(B-V)=0.2


TARGNUM:                 4
   NAME_1:               M81-OFFSET
   DESCR_1:              A
   POS_1:                RA-OFF= 0.05S +/- 1',
   POS_2:                DEC-OFF= 0' +/- 1,
   POS_3:                FROM 3,
   POS_4:                TBD-EARLY
   COMMENT_1:            TO BE FOUND - OFFSET STAR.


TARGNUM:                 5
   NAME_1:               BRIGHT_STAR
   DESCR_1:              A,111
   POS_1:                RA= 2H 16M 28S +/- 1",
   POS_2:                DEC= +43D 51' 56" +/- 2"
   EQUINOX:              1950
   FLUXNUM_1:            1
   FLUXVAL_1:            V=14,TYPE=B3V,E(B-V)=0.5
```

```
RGNUM:          6
NAME_1:         AE-AQR
DESCR_1:        A,151,154,161
POS_1:          RA= 20H 40M 9.02S +/- 0.5",
POS_2:          DEC= -0D 52' 15.5" +/- 0.5",
POS_3:          PLATE-ID=02C4
EQUINOX:        J2000
PM_OR_PAR:      N
FLUXNUM_1:      1
FLUXVAL_1:      V= 10.8 +/- 1.1


TARGNUM:        7
NAME_1:         0405-123
DESCR_1:        E,314
POS_1:          RA= 4H 5M 27.45S +/- 1",
POS_2:          DEC= -12D 19' 31.8" +/- 1"
EQUINOX:        1950
FLUXNUM_1:      1
FLUXVAL_1:      V=14.82

TARGNUM:        8
NAME_1:         MRK421
DESCR_1:        E,316
POS_1:          RA= 11H 1M 40.57S +/- 1",
POS_2:          DEC= +38D 28' 43" +/- 1"
EQUINOX:        1950
FLUXNUM_1:      1
FLUXVAL_1:      V=13.5

!
    TARGNUM:        9
    NAME_1:         WD0501+527
    NAME_2:         G191-B2B
    NAME_3:         GSSS3734-0506
    DESCR_1:        J,705,702
    POS_1:          RA=05H 05M 30.6S +/- 0.01S,
    POS_2:          DEC=+52D 49' 54.0" +/- 0.2"
    EQUINOX:        2000
    PM_OR_PAR:      Y
    POS_EPOCH_BJ:   J
    POS_EPOCH_YR:   1983.10
    RA_PM_VAL:      0.0075
    RA_PM_UNCT:     0.0050
    DEC_PM_VAL:     -0.0880
    DEC_PM_UNCT:    0.0050
    COMMENT_1:      THE GUIDE STAR CATALOG NAME
    COMMENT_2:      IS GIVEN.
    FLUXNUM_1:      1
    FLUXVAL_1:      V = 11.78 +/- 0.02
    FLUXNUM_2:      2
    FLUXVAL_2:      B = 11.44 +/- 0.02
    FLUXNUM_3:      3
    FLUXVAL_3:      U = 10.24 +/- 0.02

!
```

```
EXPOSURE_LOGSHEET:

 LINENUM:                    1.000
   TARGNAME:                 3C298-OFFSET
   CONFIG:                   FOS/RD
   OPMODE:                   ACQ/BINARY
   APERTURE:                 4.3
   SP_ELEMENT:               MIRROR
   NUM_EXP:                  1
   TIME_PER_EXP:             2.41S
   FLUXNUM_1:                1
   PRIORITY:                 3
   REQ_1:                    ONBOARD ACQ FOR 2;
   REQ_2:                    CYCLE 4 / 1-15;


 LINENUM:                    2.000
   TARGNAME:                 3C298
   CONFIG:                   FOS/RD
   OPMODE:                   ACCUM
   APERTURE:                 0.5
   SP_ELEMENT:               G780H
   WAVELENGTH:               7800
   NUM_EXP:                  1
   TIME_PER_EXP:             600S
   S_TO_N:                   10
   FLUXNUM_1:                1
   PRIORITY:                 3
   COMMENT_1:                SIGNAL_TO_NOISE
   COMMENT_2:                IS PER DIODE.

 LINENUM:                    3.000
   TARGNAME:                 MRK421
   CONFIG:                   FOS/RD
   OPMODE:                   ACQ/BINARY
   APERTURE:                 4.3
   SP_ELEMENT:               MIRROR
   PARAM_1:                  BRIGHT=57500,
   PARAM_2:                  FAINT=1100,
   NUM_EXP:                  1
   TIME_PER_EXP:             0.66S
   FLUXNUM_1:                1
   PRIORITY:                 3
   REQ_1:                    ONBOARD ACQ FOR 4;
   REQ_2:                    GROUP 3-4.3 NO GAP;
   COMMENT_1:                BLUE SIDE ACQ BIN- EXP=0.83
   COMMENT_2:                SEC. USE DEFAULT BRIGHT
   COMMENT_3:                AND FAINT LIMITS.
```

```
LINENUM:                    4.000
  TARGNAME:                 MRK421
  CONFIG:                   FOS/RD
  OPMODE:                   ACQ/PEAK
  APERTURE:                 0.25x2.0
  SP_ELEMENT:               G190H
  NUM_EXP:                  1
  TIME_PER_EXP:             0.3S
  PRIORITY:                 1
  PARAM_1:                  SCAN-STEP-X=.057,
  PARAM_2:                  SEARCH-SIZE-X=7,
  PARAM_3:                  SEARCH-SIZE-Y=1,
  REQ_1:                    ONBOARD ACQ FOR 4.1-4.3;

LINENUM:                    4.100
  TARGNAME:                 MRK421
  CONFIG:                   FOS/RD
  OPMODE:                   ACCUM
  APERTURE:                 0.25X2.0
  SP_ELEMENT:               G190H
  NUM_EXP:                  1
  TIME_PER_EXP:             300S
  PRIORITY:                 1

LINENUM:                    4.200
  TARGNAME:                 MRK421
  CONFIG:                   FOS/BL
  OPMODE:                   ACQ/PEAK
  APERTURE:                 0.25x2.0
  SP_ELEMENT:               G190H
  NUM_EXP:                  1
  TIME_PER_EXP:             0.6S
  PRIORITY:                 1
  PARAM_1:                  SCAN-STEP-X=.057,
  PARAM_2:                  SEARCH-SIZE-X=7,
  PARAM_3:                  SEARCH-SIZE-Y=1,
  REQ_1:                    ONBOARD ACQ FOR 4.3;

LINENUM:                    4.300
  TARGNAME:                 MRK421
  CONFIG:                   FOS/BL
  OPMODE:                   ACCUM
  APERTURE:                 0.25X2.0
  SP_ELEMENT:               G130H
  NUM_EXP:                  1
  TIME_PER_EXP:             300S
  PRIORITY:                 1

LINENUM:                    5.000
  TARGNAME:                 M81
  CONFIG:                   WFC
  OPMODE:                   IMAGE
  APERTURE:                 ALL
  SP_ELEMENT:               F606W
  NUM_EXP:                  1
  TIME_PER_EXP:             60S
  FLUXNUM_1:                1
  PRIORITY:                 1
  REQ_1:                    EARLY ACQ FOR 6-8.1;
```

```
LINENUM:                    6.000
  TARGNAME:                 M81-OFFSET
  CONFIG:                   FOS/BL
  OPMODE:                   ACQ/BINARY
  APERTURE:                 4.3
  SP_ELEMENT:               MIRROR
  NUM_EXP:                  1
  TIME_PER_EXP:             TBD
  FLUXNUM_1:                1
  PRIORITY:                 1
  REQ_1:                    SEQ 6-8.1 NO GAP;
  REQ_2:                    ONBOARD ACQ FOR 7-8.1;

LINENUM:                    7.000
  TARGNAME:                 M81
  CONFIG:                   FOS/BL
  OPMODE:                   ACCUM
  APERTURE:                 0.3
  SP_ELEMENT:               G190H
  WAVELENGTH:               1900
  NUM_EXP:                  1
  TIME_PER_EXP:             3000S
  FLUXNUM_1:                1
  PRIORITY:                 1
  S_TO_N:                   10
  COMMENT_1:                SIGNAL_TO_NOISE
  COMMENT_2:                IS PER DIODE.

LINENUM:                    8.000
  TARGNAME:                 M81
  CONFIG:                   FOS/BL
  OPMODE:                   ACQ
  APERTURE:                 4.3
  SP_ELEMENT:               MIRROR
  NUM_EXP:                  1
  TIME_PER_EXP:             200S
  FLUXNUM_1:                1
  PRIORITY:                 1
  COMMENT_1:                FOS ACQIMAGE OF FIELD OF
  COMMENT_2:                VIEW.

LINENUM:                    8.100
  TARGNAME:                 M81
  CONFIG:                   FOS/BL
  OPMODE:                   IMAGE
  APERTURE:                 0.3
  SP_ELEMENT:               G400H
  NUM_EXP:                  1
  TIME_PER_EXP:             3600S
  S_TO_N:                   10
  PRIORITY:                 1
  PARAM_1:                  Y-SIZE=3,
  PARAM_2:                  Y-SPACE=10.7,
  PARAM_3:                  COMB=YES,
  PARAM_4:                  SUB-STEP=4,
  COMMENT_1:                SIGNAL_TO_NOISE
  COMMENT_2:                IS PER PIXEL.
```

```
LINENUM:                10.300
  TARGNAME:              BRIGHT_STAR
  CONFIG:                FOS/RD
  OPMODE:                ACQ/PEAK
  APERTURE:              4.3
  SP_ELEMENT:            G570H
  WAVELENGTH:            5700
  NUM_EXP:               1
  TIME_PER_EXP:          0.17S
  PRIORITY:              1
  PARAM_1:               SCAN-STEP-Y=1.204,
  PARAM_2:               SEARCH-SIZE-X=1,
  PARAM_3:               SEARCH-SIZE-Y=3,
  REQ_1:                 ONBOARD ACQ FOR 10.4;

LINENUM:                10.400
  TARGNAME:              BRIGHT_STAR
  CONFIG:                FOS/RD
  OPMODE:                ACQ/PEAK
  APERTURE:              1.0
  SP_ELEMENT:            G570H
  WAVELENGTH:            5700
  NUM_EXP:               1
  TIME_PER_EXP:          0.18S
  PRIORITY:              1
  PARAM_1:               SCAN-STEP-X=.602,
  PARAM_2:               SCAN-STEP-Y=.301,
  PARAM_3:               SEARCH-SIZE-X=6,
  PARAM_4:               SEARCH-SIZE-Y=2,
  REQ_1:                 ONBOARD ACQ FOR 10.5;

LINENUM:                10.500
  TARGNAME:              BRIGHT_STAR
  CONFIG:                FOS/RD
  OPMODE:                ACQ/PEAK
  APERTURE:              0.5
  SP_ELEMENT:            G570H
  WAVELENGTH:            5700
  PARAM_1:               SCAN-STEP-X=0.30,
  PARAM_2:               SCAN-STEP-Y=0.30,
  PARAM_3:               SEARCH-SIZE-X=3,
  PARAM_4:               SEARCH-SIZE-Y=3,
  NUM_EXP:               1
  TIME_PER_EXP:          0.19S
  PRIORITY:              1
  REQ_1:                 ONBOARD ACQ FOR 10.6;


LINENUM:                10.600
  TARGNAME:              BRIGHT_STAR
  CONFIG:                FOS/RD
  OPMODE:                ACCUM
  APERTURE:              1.0
  SP_ELEMENT:            G570H
  WAVELENGTH:            5700
  NUM_EXP:               1
  TIME_PER_EXP:          1M
  PRIORITY:              1
```

```
LINENUM:                    11.000
  TARGNAME:                 AE-AQR
  CONFIG:                   FOS/BL
  OPMODE:                   ACQ/PEAK
  APERTURE:                 4.3
  SP_ELEMENT:               G190H
  NUM_EXP:                  1
  TIME_PER_EXP:             0.07S
  FLUXNUM_1:                1
  PRIORITY:                 1
  PARAM_1:                  SCAN-STEP-Y=1.204,
  PARAM_2:                  SEARCH-SIZE-X=1,
  PARAM_3:                  SEARCH-SIZE-Y=3,
  REQ_1:                    ONBOARD ACQ FOR 11.1;
  COMMENT_1:                VARIABLE TARGET. FAINTEST
  COMMENT_2:                V MAG USED WITH 13,000 BB
  COMMENT_3:                IN SIMULATION. EXPECT MIN
  COMMENT_4:                1000 COUNTS/DWELL.

LINENUM:                    11.100
  TARGNAME:                 AE-AQR
  CONFIG:                   FOS/BL
  OPMODE:                   ACQ/PEAK
  APERTURE:                 1.0
  SP_ELEMENT:               G190H
  NUM_EXP:                  1
  TIME_PER_EXP:             0.08S
  FLUXNUM_1:                1
  PRIORITY:                 1
  PARAM_1:                  SCAN-STEP-X=.602,
  PARAM_2:                  SCAN-STEP-Y=.301,   .602
  PARAM_3:                  SEARCH-SIZE-X=6,
  PARAM_4:                  SEARCH-SIZE-Y=2,
  REQ_1:                    ONBOARD ACQ FOR 11.2;

LINENUM:                    11.200
  TARGNAME:                 AE-AQR
  CONFIG:                   FOS/BL
  OPMODE:                   ACQ/PEAK
  APERTURE:                 0.3
  SP_ELEMENT:               G190H
  NUM_EXP:                  1
  TIME_PER_EXP:             0.09S
  FLUXNUM_1:                1
  PRIORITY:                 1
  PARAM_1:                  SEARCH-SIZE=4,
  PARAM_2:                  SCAN-STEP=0.25,
  REQ_1:                    ONBOARD ACQ FOR 11.3;
```

```
LINENUM:                    11.300
  TARGNAME:                 AE-AQR
  CONFIG:                   FOS/BL
  OPMODE:                   ACQ/PEAK
  APERTURE:                 0.3
  SP_ELEMENT:               G190H
  NUM_EXP:                  1
  TIME_PER_EXP:             0.90S
  FLUXNUM_1:                1
  PRIORITY:                 1
  PARAM_1:                  SEARCH-SIZE-X=5,
  PARAM_2:                  SEARCH-SIZE-Y=5,
  PARAM_3:                  SCAN-STEP-X=0.06,
  PARAM_4:                  SCAN-STEP-Y=0.06,
  REQ_1:                    ONBOARD ACQ FOR 12;
  COMMENT_1:                CRITICAL ACQ/PEAK STAGE.
  COMMENT_2:                EXP TO PRODUCE 10000
  COMMENT_3:                COUNTS/DWELL.

LINENUM:                    12.000
  TARGNAME:                 AE-AQR
  CONFIG:                   FOS/BL
  OPMODE:                   RAPID
  APERTURE:                 0.3
  SP_ELEMENT:               G190H
  NUM_EXP:                  1
  TIME_PER_EXP:             300M
  PRIORITY:                 1
  PARAM_1:                  READ-TIME=4,

LINENUM:                    13.000
  TARGNAME:                 WD0501+527
  CONFIG:                   FOS/RD
  OPMODE:                   ACQ/PEAK
  APERTURE:                 4.3
  SP_ELEMENT:               G270H
  NUM_EXP:                  1
  TIME_PER_EXP:             3.0S
  PRIORITY:                 1
  PARAM_1:                  SCAN-STEP-Y=1.204,
  PARAM_2:                  SEARCH-SIZE-X=1,
  PARAM_3:                  SEARCH-SIZE-Y=3,
  REQ_1:                    ONBOARD ACQ FOR 13.1;

LINENUM:                    13.100
  TARGNAME:                 WD0501+527
  CONFIG:                   FOS/RD
  OPMODE:                   ACQ/PEAK
  APERTURE:                 1.0
  SP_ELEMENT:               G270H
  NUM_EXP:                  1
  TIME_PER_EXP:             3.0S
  PRIORITY:                 1
  PARAM_1:                  SCAN-STEP-X=.602,
  PARAM_2:                  SCAN-STEP-Y=.301,
  PARAM_3:                  SEARCH-SIZE-X=6,
  PARAM_4:                  SEARCH-SIZE-Y=2,
  REQ_1:                    ONBOARD ACQ FOR 13.2;
```

.602

```
LINENUM:                13.200
  TARGNAME:             WD0501+527
  CONFIG:               FOS/RD
  OPMODE:               ACQ/PEAK
  APERTURE:             0.5
  SP_ELEMENT:           G270H
  NUM_EXP:              1
  TIME_PER_EXP:         3.0S
  FLUXNUM_1:            1
  PRIORITY:             1
  PARAM_1:              SEARCH-SIZE-X=3,
  PARAM_2:              SEARCH-SIZE-Y=3,
  PARAM_3:              SCAN-STEP-X=0.30
  PARAM_4:              SCAN-STEP-Y=0.30
  REQ_1:                ONBOARD ACQ FOR 13.3;

LINENUM:                13.300
  TARGNAME:             WD0501+527
  CONFIG:               FOS/RD
  OPMODE:               ACQ/PEAK
  APERTURE:             0.3
  SP_ELEMENT:           G270H
  NUM_EXP:              1
  TIME_PER_EXP:         3.0S
  FLUXNUM_1:            1
  PRIORITY:             1
  PARAM_1:              SEARCH-SIZE-X=4,
  PARAM_2:              SEARCH-SIZE-Y=4,
  PARAM_3:              SCAN-STEP-X=0.125,
  PARAM_4:              SCAN-STEP-Y=0.125,
  REQ_1:                ONBOARD ACQ FOR 13.4;

LINENUM:                13.400
  TARGNAME:             WD0501+527
  CONFIG:               FOS/RD
  OPMODE:               ACCUM
  APERTURE:             0.5
  SP_ELEMENT:           G270H
  NUM_EXP:              1
  TIME_PER_EXP:         276S
  PRIORITY:             1

LINENUM:                14.000
  TARGNAME:             0405-123
  CONFIG:               FOS/BL
  OPMODE:               ACQ/BINARY
  APERTURE:             4.3
  SP_ELEMENT:           MIRROR
  NUM_EXP:              1
  TIME_PER_EXP:         2.8S
  S_TO_N:               17
  FLUXNUM_1:            1
  FLUXNUM_2:            3
  PRIORITY:             1
  REQ_1:                ONBOARD ACQ FOR 15;
  REQ_2:                SEQ 14-15 NO GAP;
```

```
INENUM:                 15.000
TARGNAME:               0405-123
CONFIG:                 FOS/BL
OPMODE:                 ACCUM
APERTURE:               4.3
SP_ELEMENT:             G270H
WAVELENGTH:             2700
PARAM_1:                POLSCAN=4B
NUM_EXP:                1
TIME_PER_EXP:           5H
S_TO_N:                 90
FLUXNUM_1:              1
FLUXNUM_2:              3
PRIORITY:               1
```